Optics Measurement Techniques for Transfer Line & Beam Instrumentation

CAS for Beam Injection, Extraction and Transfer Line
Erice, 16th and 17th of March 2017

Peter Forck

Gesellschaft für Schwerionenforschnung (GSI) and University Frankfurt

2nd part of this lecture covers:

- Transverse profile measurement techniques at transfer line and synchrotron
  Application: transverse matching to synchrotron
- Emittance determination and transfer lines

The beam width can be changed by focusing via quadruples.

Transverse matching between ascending accelerators is done by focusing.

$\longrightarrow$ Profiles have to be controlled at many locations.

Synchrotrons: Lattice functions $\boldsymbol{\beta(s)}$ and ***D(s)*** are fixed $\Rightarrow$ width $\boldsymbol{\sigma}$ and emittance $\boldsymbol{\varepsilon}$ are:

$$\sigma_x^2(s) = \varepsilon_x \beta_x(s) + \left(D(s) \frac{\Delta p}{p} \right)^2 \quad \text{and} \quad \sigma_y^2(s) = \varepsilon_y \beta_y(s) \qquad \text{(no vertical bend)}$$

Transfer lines: Lattice functions are 'smoothly' defined due to variable input emittance.

Typical beam sizes:

e^--beam: typically Ø 0.1 to 3 mm, **protons:** typically Ø 1 to 30 mm

A great variety of devices are used:

- ***Optical techniques***: Scintillating screens (all beams), synchrotron light monitors (e−), optical transition radiation (e−, high energetic p), ionization profile monitors (protons)
- ***Electronics techniques:*** Secondary electron emission SEM grids, wire scanners (all)

Scintillation Screen

Particle's energy loss in matter produces light
→ the most direct way of profile observation as used from the early days on!

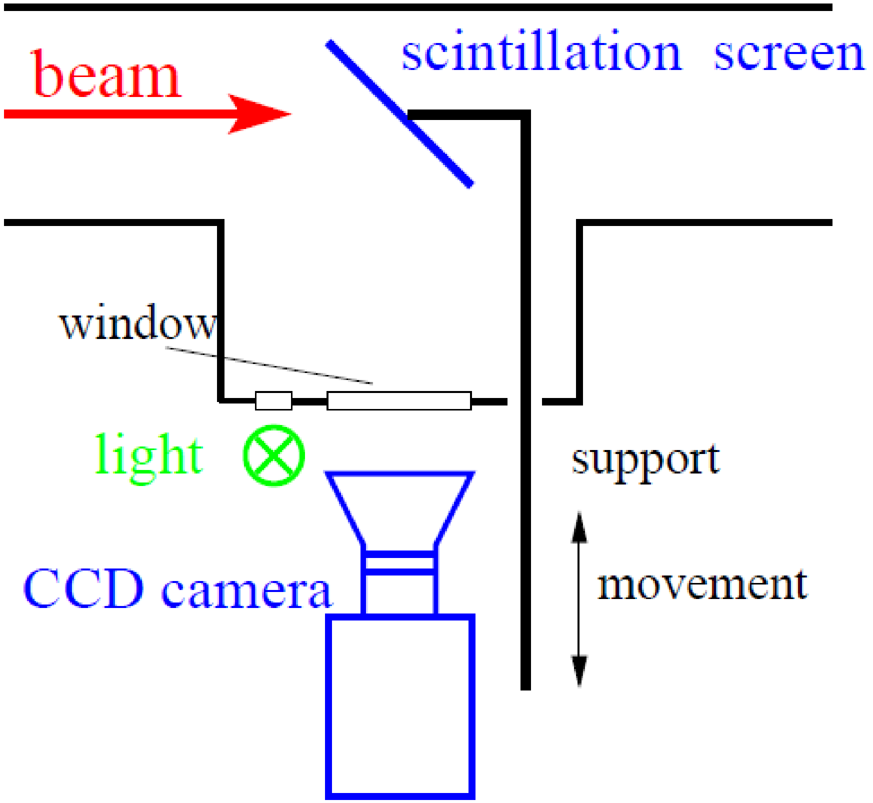

Pneumatic feed-through with Ø70 mm screen :

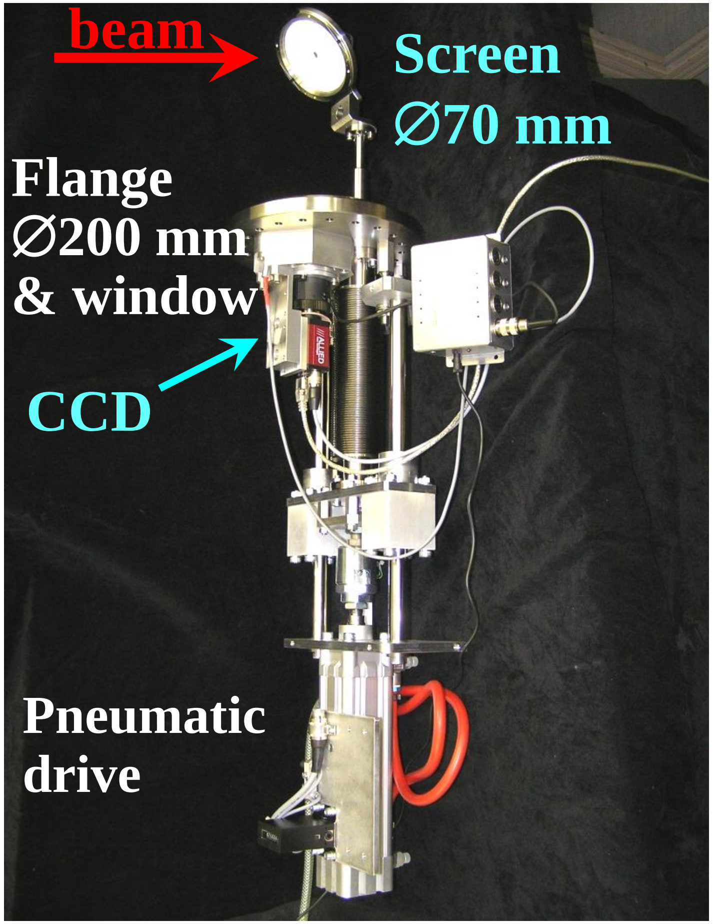

Example of Screen based Beam Profile Measurement

Example: GSI LINAC, 4 MeV/u, low current, YAG:Ce screen

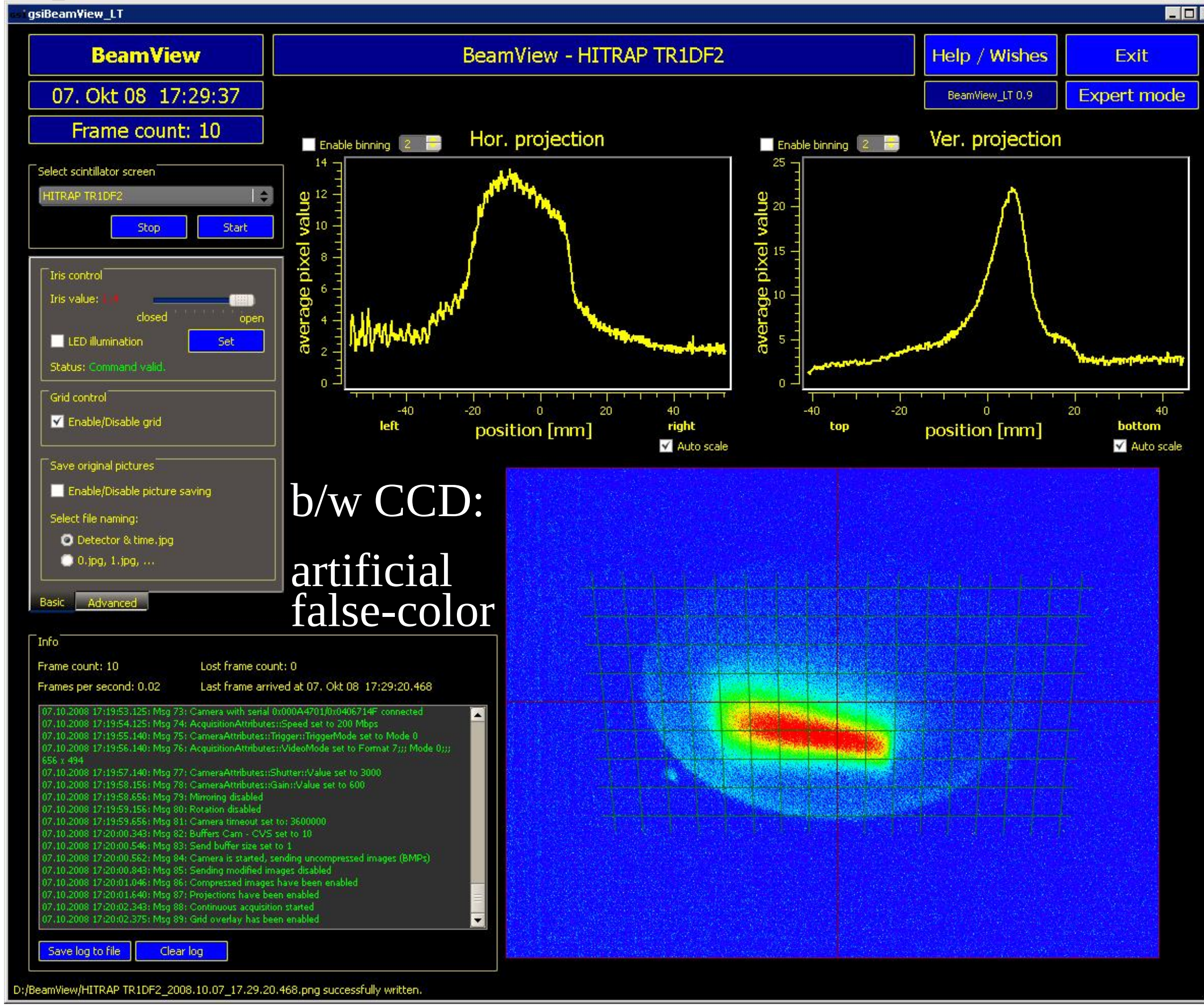

Advantage of screens:

- ➢Direct 2-dim measurement
- ➢High spatial resolution
- ➢Cheap realization

⇒ widely used at transfer lines

Disadvantage of screens:

- ➢Intercepting device
- ➢ Some material might brittle
- ➢ Low dynamic range
- ➢Might be destroyed by the beam

Observation with
a CCD, CMOS or video camera

Scintillation Screen (beam stopped)

First turn diagnostics:

Synchrotron acts as a transport line as 1st step of commissioning

- Current measurement with Faraday Cup or transformer or BPM
- Profile measurement with Screens, SEM-Grid or OTR

Installation: at injection, after one turn & sometimes after each 'sector' for malfunction diagnostics

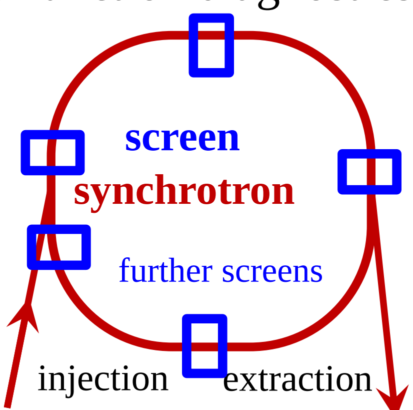

Historical Example & CAS poster:

First turn at CERN LHC on September 10th, 2008

Protons 450 GeV, Al_2O_3:Cr screen mounted after injection

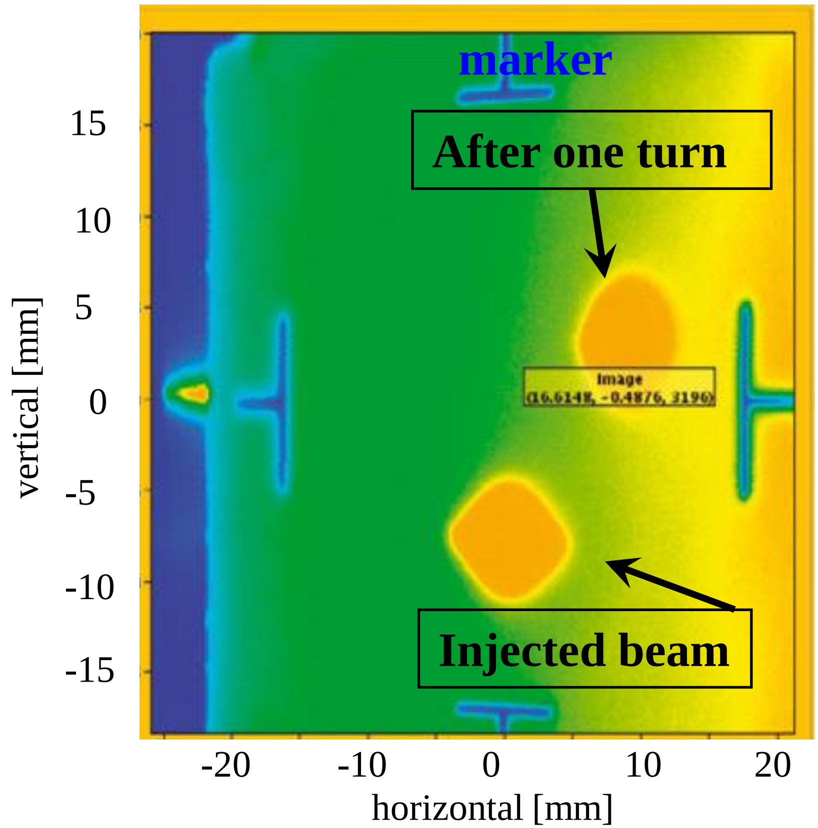

CERN Logbook on Sep. 10th, 2008: It's 10.26 a.m. and the screen in the CCC shows the two spots that indicate that beam has for the first time made a complete circuit of the LHC.

Direct measurement of position and beam distribution of extracted beam by a screen

Example: Test of emergency kicker at LHC (from CAS poster)

→ascending stored bunches are dumped at different locations to prevent for over-heating

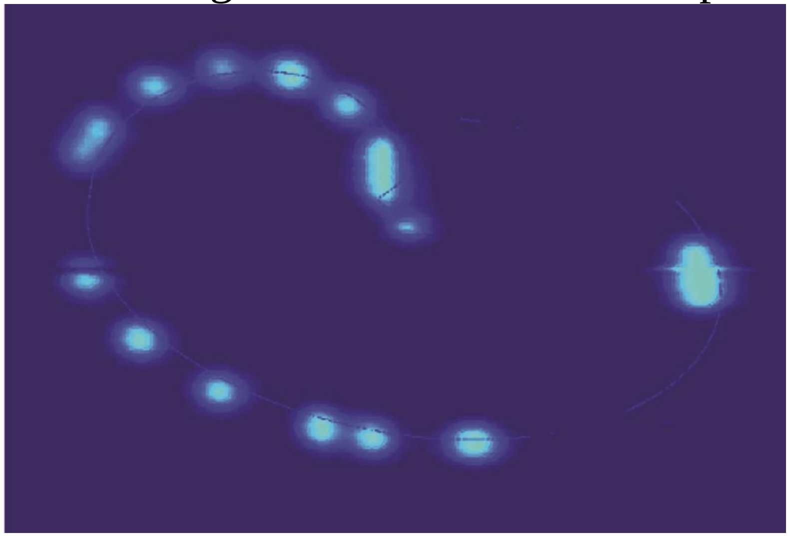

LHC emergency dump diagnostics by Al_2O_3:Cr

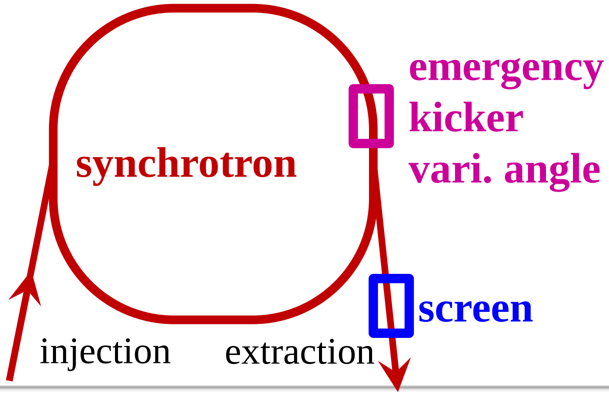

Example: Color CCD camera: Images at different particle intensities determined for U at 300 MeV/u

Al_2O_3

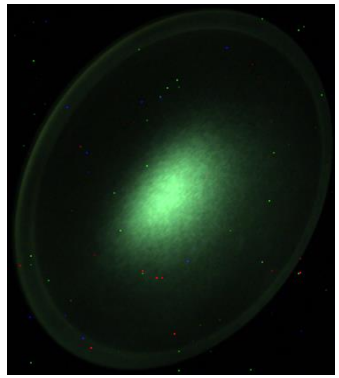

CsI:Tl

Al_2O_3:Cr

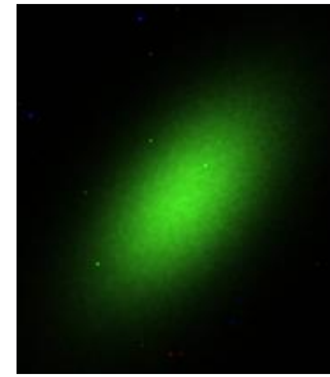

P43

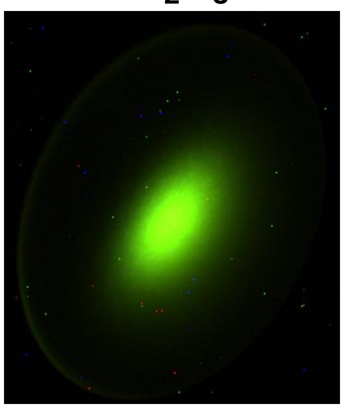

YAG:Ce

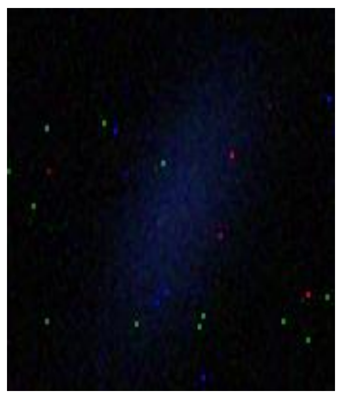

Herasil

Quartz:Ce

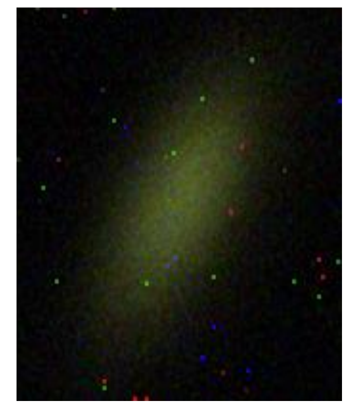

ZrO_2:Mg

- ➢ Very different light yield i.e. photons per ion‘s energy loss
- ➢ Different wavelength of emitted light

Material Properties for Scintillating Screens

Some materials and their basic properties:

Name	Type	Material	Activ.	Max. λ	Decay
Chromox	Cera-mics	Al_2O_3	Cr	700 nm	≈ 10 ms
Alumina		Al_2O_3	Non	380 nm	≈ 10 ns
YAG:Ce	Crystal	$Y_3Al_5O_{12}$	Ce	550 nm	200 ns
LuAG:Ce		$Lu_3Al_5O_{12}$	Ce	535 nm	70 ns
P43	Powder	Gd_2O_3S	Tb	545 nm	1 ms
P46		$Y_3Al_5O_{12}$	Ce	530 nm	300 ns
P47		$Y_3Si_5O_{12}$	Ce&Tb	400 nm	100 ns

Standard drive with P43 screen

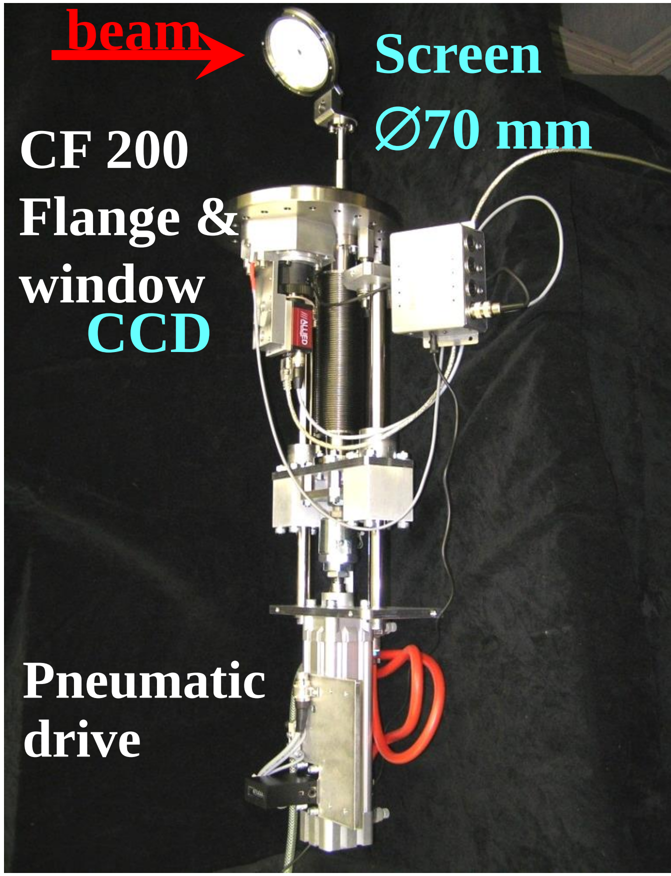

Properties of a good scintillator:

- Light output at optical wavelength for standard camera
- Large dynamic range → usable for different ions
- Short decay time → observation of variations
- Radiation hardness → long lifetime
- Good mechanical properties → typ. size up to Ø 10 cm

(Phosphor Pxx grains of Ø ≈ 10 μm on glass or metal).

Example: Light Output from various Screens

Example: Beam images for various scintillators irradiated by Uranium at ≈ 300 MeV/u at GSI

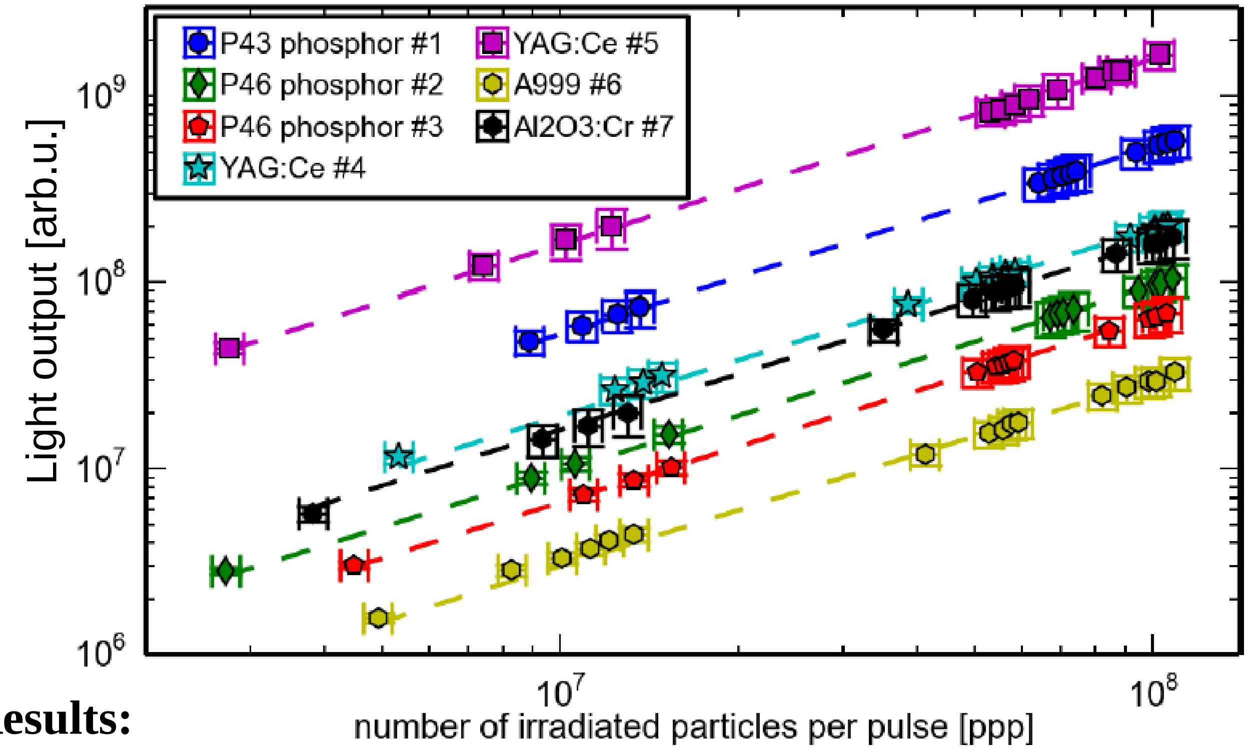

Courtesy P. Forck et al., IPAC'14,
A. Lieberwirth et al., NIM B 2015

Results:

- Several orders of magnitude different light output
- ⇒ material matched to beam intensity must be chosen
- Well suited: powder phosphor screens P43 and P46
- → cheap, can be sedimented on large substrates of nearly any shape
- Light output linear with respect to particles per pulse

Outline:

- Scintillation screens:

  emission of light, universal usage, limited dynamic range
- SEM-Grid: emission of electrons, workhorse, limited resolution

  Multi Wire Proportional Chamber for slow extr. : gas ionization, limited resol.
- Wire scanner
- Ionization Profile Monitor
- Optical Transition Radiation
- Synchrotron Light Monitors
- Summary

Energy loss of ions in metals close to a surface:

Closed collision with large energy transfer: → fast e⁻ with E_{kin} >> 100 eV

Distant collision with low energy transfer → slow e⁻ with $E_{kin} \lesssim$ 10 eV

→ 'diffusion' & scattering with other e⁻: scattering length $L_s \approx$ 1 - 10 nm

→ at surface ≈ 90 % probability for escape

Secondary **electron yield** and energy distribution comparable for all metals!

⇒ ***Y = const. * dE/dx*** (Sternglass formula)

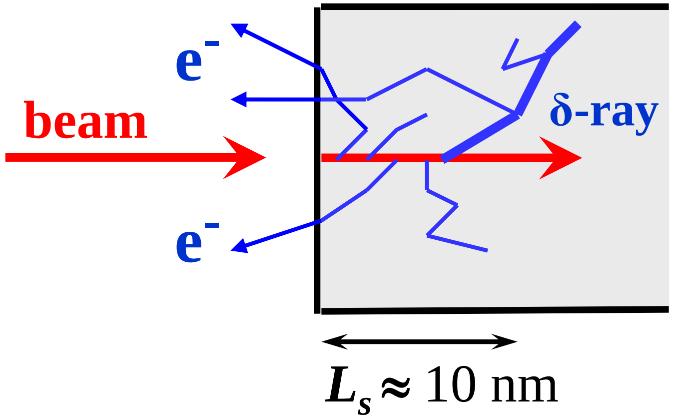

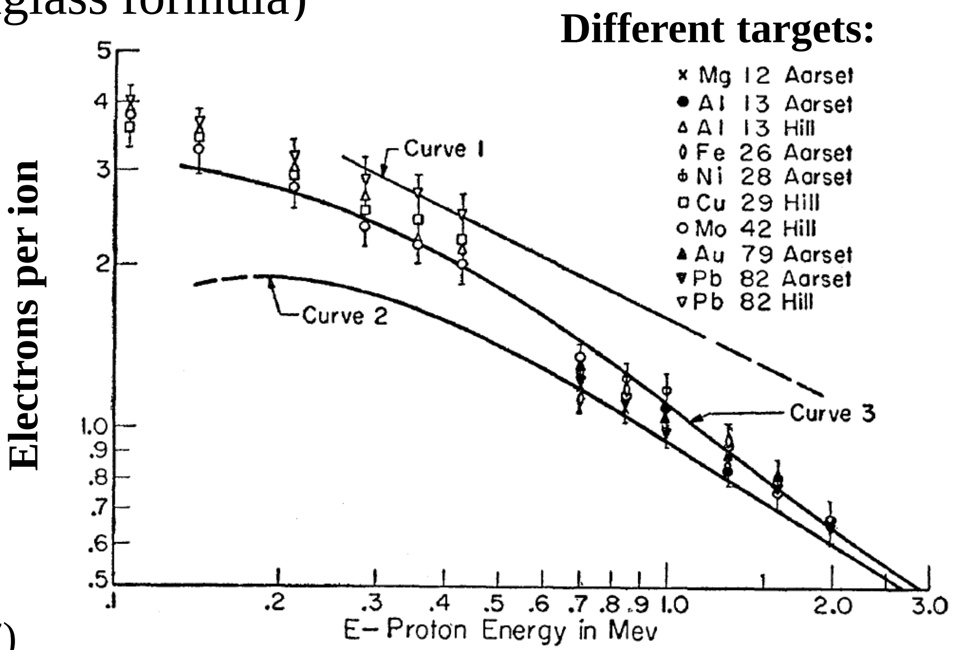

From E.J. Sternglass, Phys. Rev. 108, 1 (1957)

Beam surface interaction: e^- emission → measurement of current.

Example: 15 wire spaced by 1.5 mm:

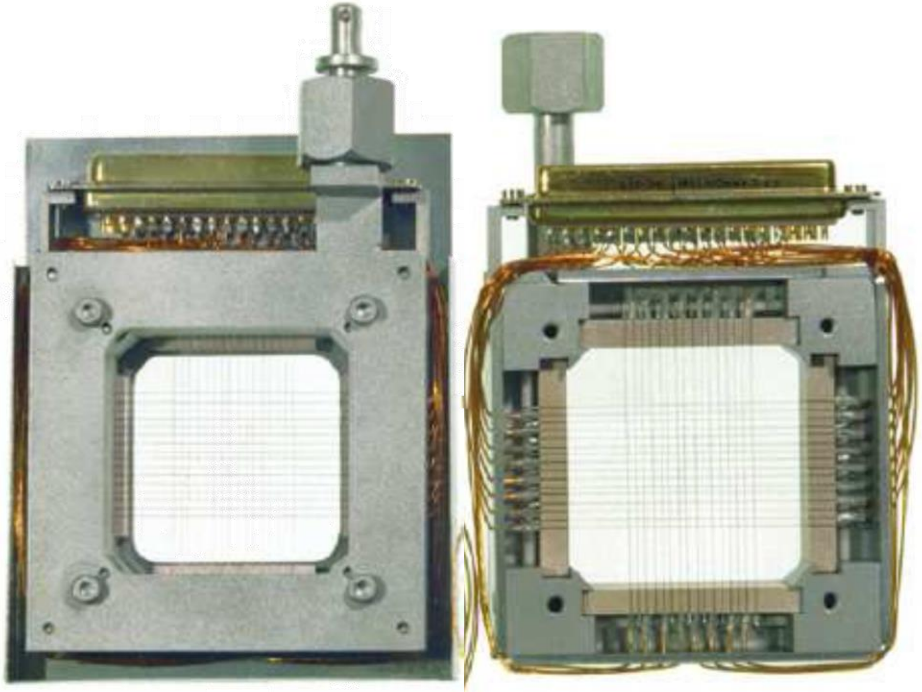

SEM-Grid feed-through on CF200:

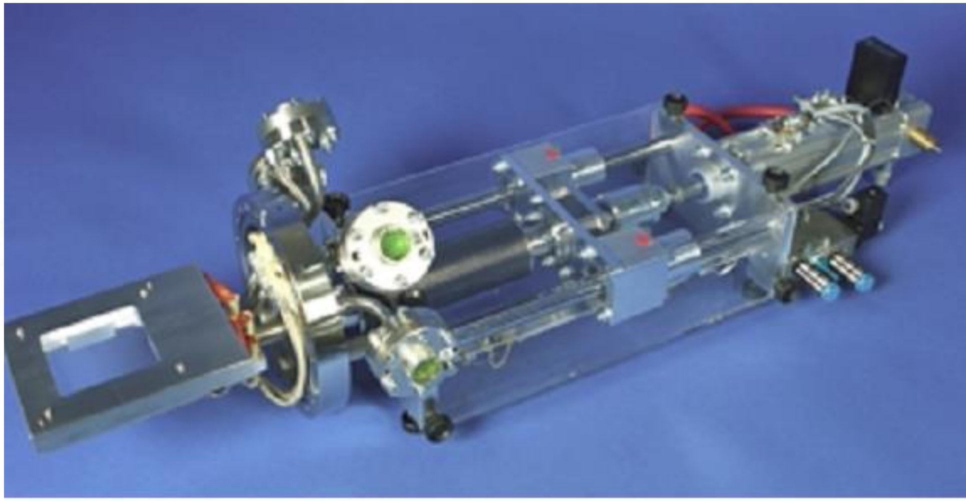

Beam surface interaction: e^- emission → measurement of current.

Example: 15 wire spaced by 1.5 mm:

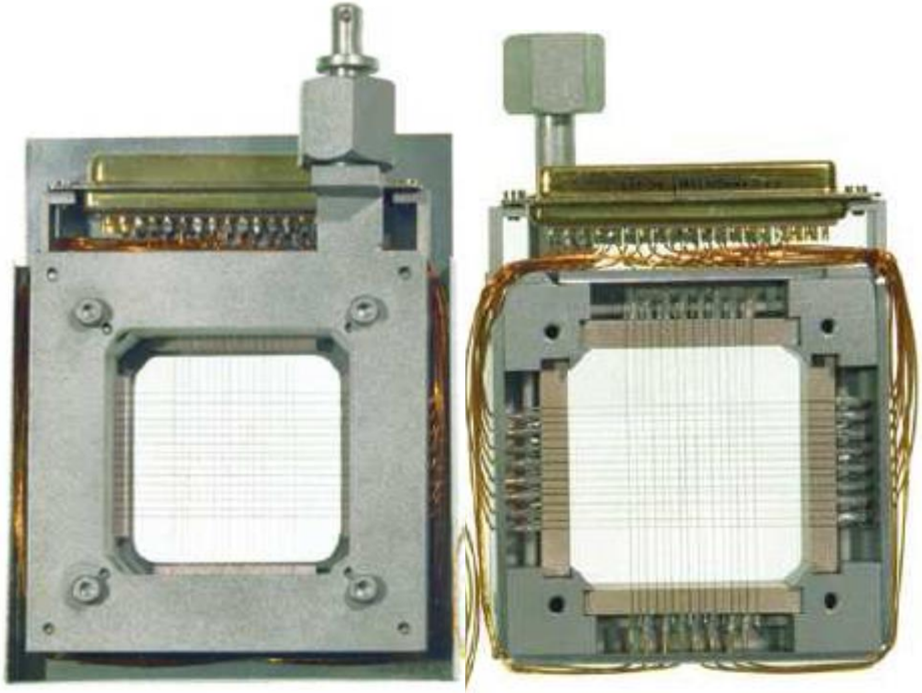

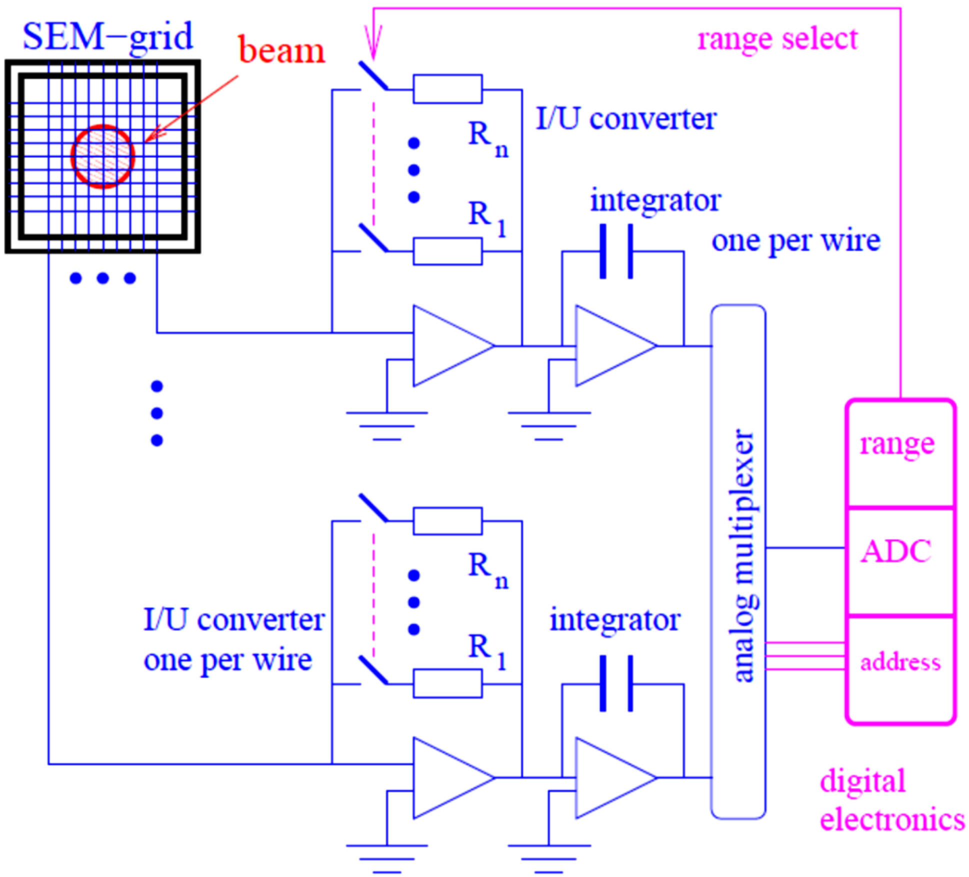

Each wire is equipped with one I/U converter
different ranges settings by R_i
→ very large dynamic range up to 10^6.

Properties of a SEM-Grid

Secondary e- emission from wire or ribbons, 10 to 100 per plane.

Specifications for SEM-Grids at the GSI-LINAC:

Diameter of the wires	0.05 to 0.5 mm
Spacing	0.5 to 2 mm
Length	50 to 100 mm
Material	W or W-Re alloy
Insulation of the frame	glass or Al_2O_3
number of wires	10 to 100
Max. power rating in vacuum	1 W/mm
Min. sensitivity of I/U-conv.	1 nA/V
Dynamic range	$1:10^6$
Number of ranges	10 typ.
Integration time	1 μs to 1 s

Example: Ribbon type SEM-Grid

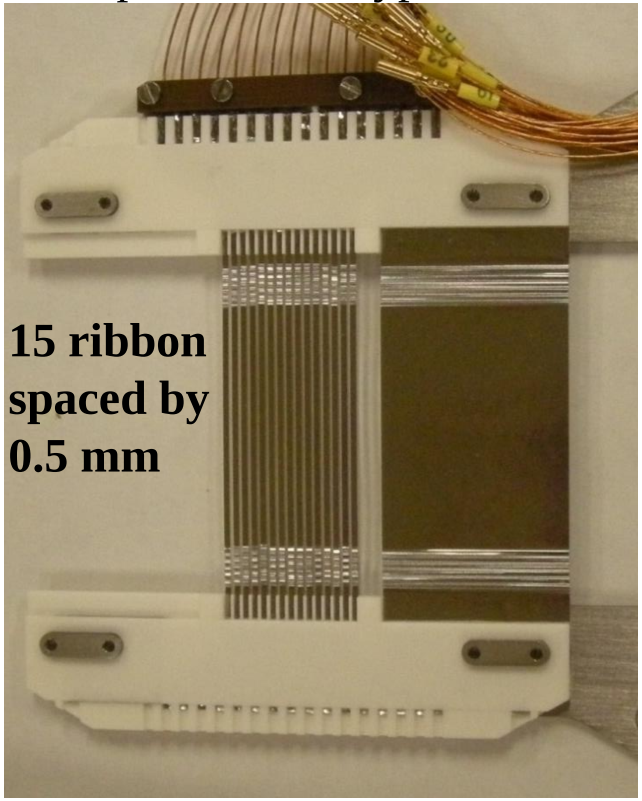

Care has to be taken to prevent over-heating by the energy loss!

Low energy beam: **Wires** with ratio of spacing/width: $\simeq$ 1mm/0.1mm = 10 $\rightarrow$ only 10 % loss.

High energy E_{kin} > 1 GeV/u: typ. 25 μm thick **ribbons** & 0.5 mm width $\rightarrow$ negligible energy loss.

Example of Profile Mesurement with SEM-Grids

Even for low energies, several SEM-Grid can be used due to the ≈80 % transmission

⇒ frequently used for beam optimization: setting of quadrupoles, energy….

SEM-Grid is installed in vacuum → for sufficient signal ***I(t)*** for fast extraction only

Example: C^{6+} beam of 11.4 MeV/u at different locations at GSI-transfer line

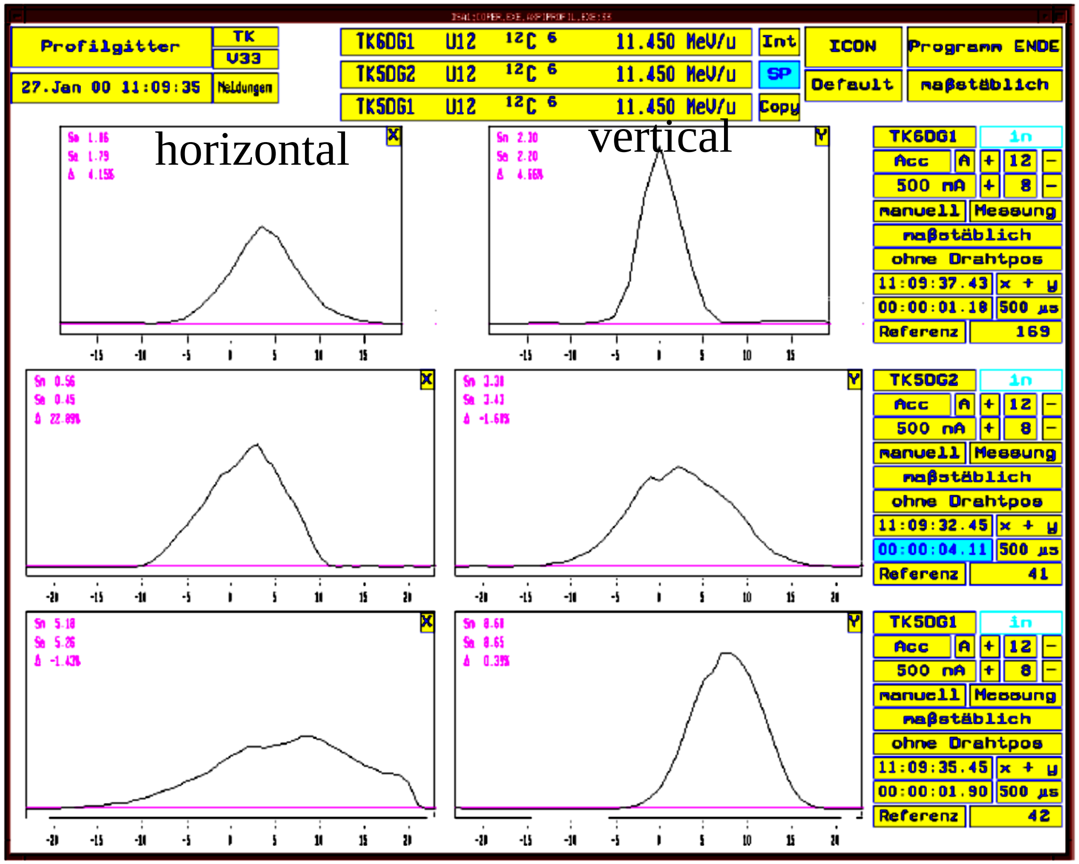

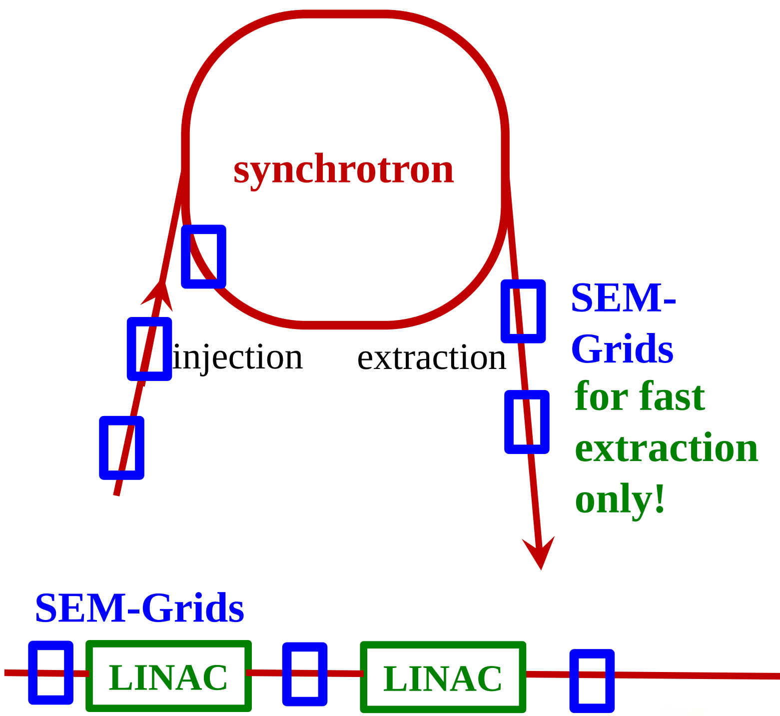

MWPC: Multi Wire Proportional Chamber

Electron avalanche due to high electric field at signal wire

Typical gas: 80 % Ar + 20 % CO_2 or CH_4

Amplification factor: 100 … 1000 compared to IC

used for slow extraction

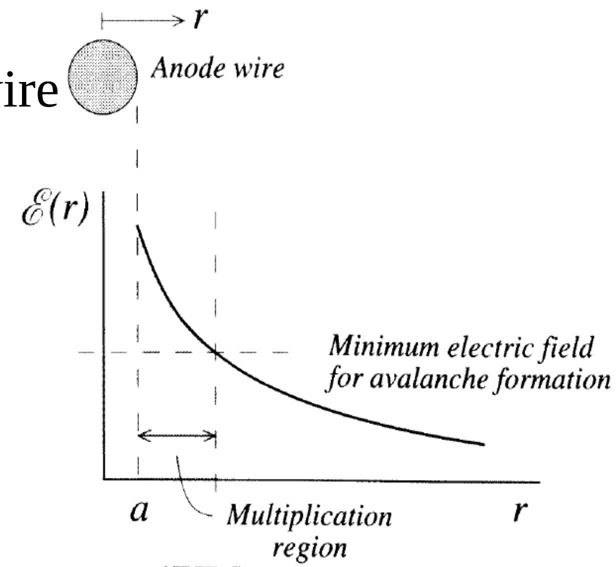

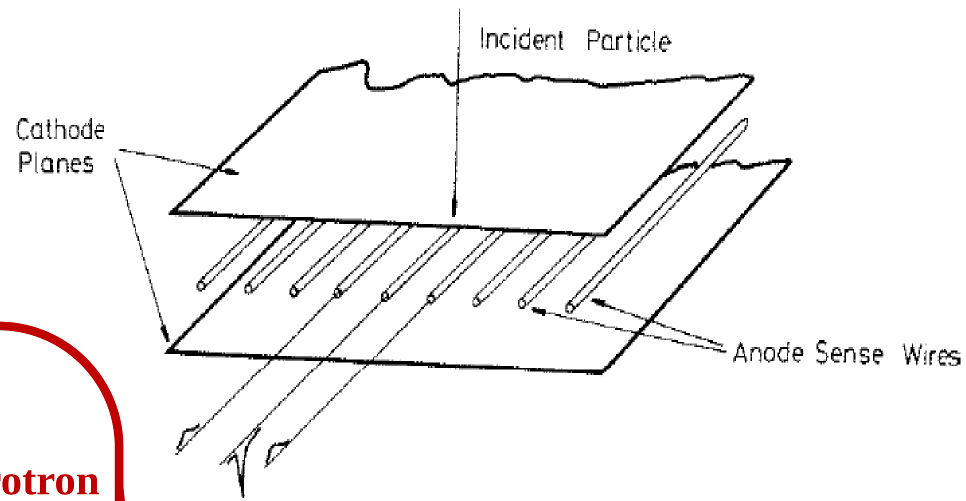

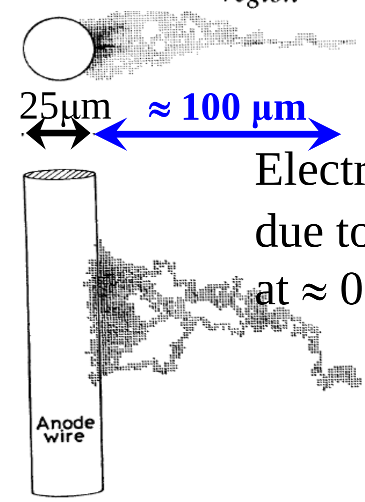

Electron avalanche due to high E-field at ≈ 0.1 mm at wire

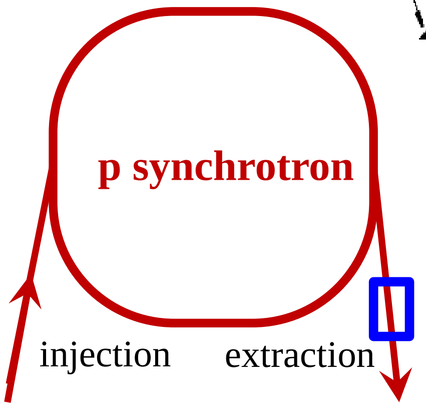

MWPC for slow extr.

MWPC: Multi Wire Proportional Chamber

Electron avalanche due to high electric field at signal wire

Typical gas: 80 % Ar + 20 % CO_2 or CH_4

Amplification factor: 100 … 1000 compared to IC

Example: Ar^{18+} at 300 MeV/u slow extraction by quadrupole variation of 2 s

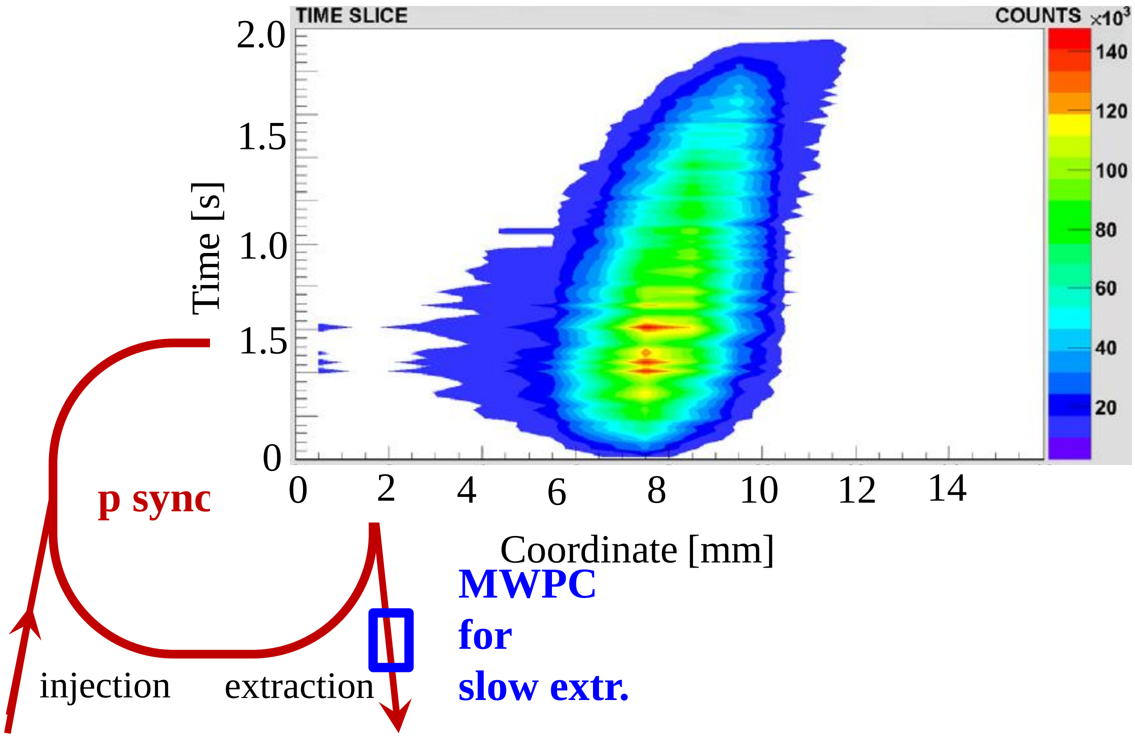

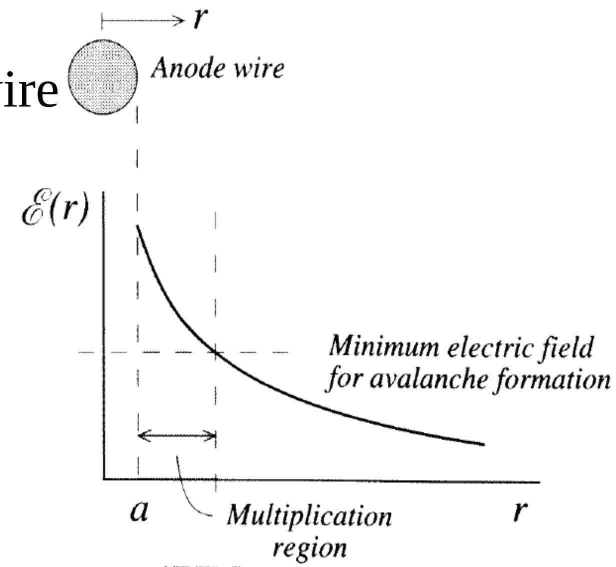

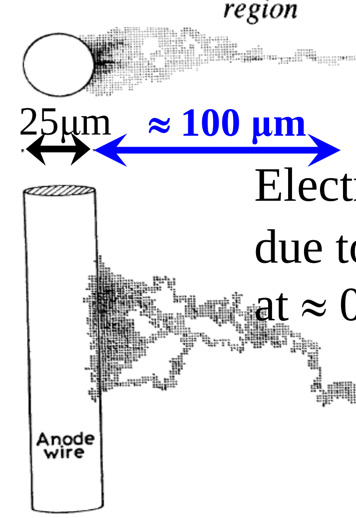

Electron avalanche due to high E-field at ≈ 0.1 mm at wire

Example of a Multi-Wire-Proportional-Chamber (MWPC)

The MWPC hardware:

- Detector head, wire spacing 1 mm (left),
- Assembly (right)
- Mechanical drive (bottom)

  with Ar + CO_2 gas-filled volume: ‘Pocket’

  → Steel window of 50 μm thickness

  → ***p*** = 1 bar pressure inside ‘pocket’

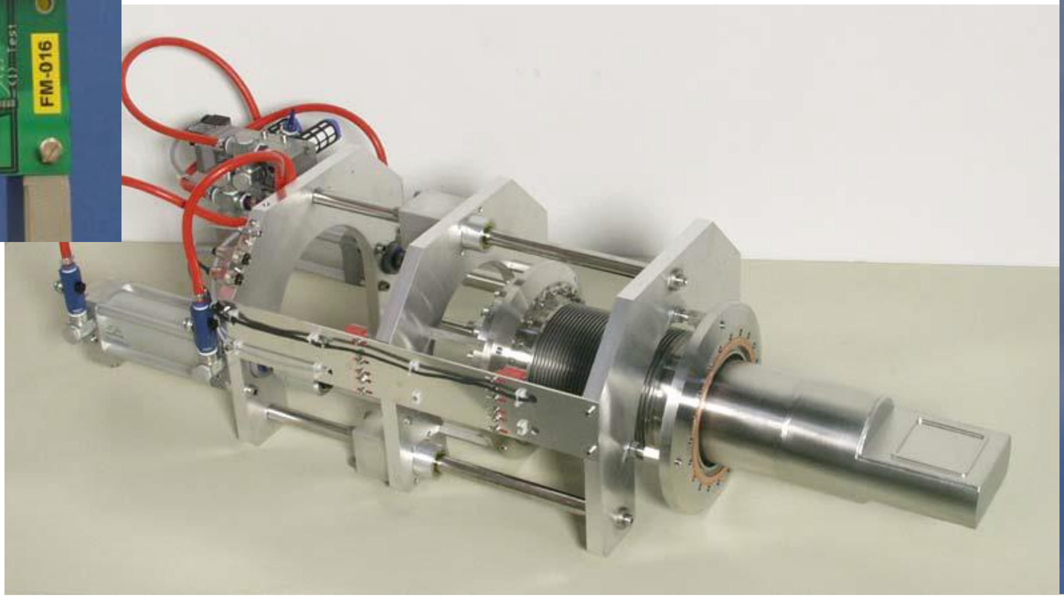

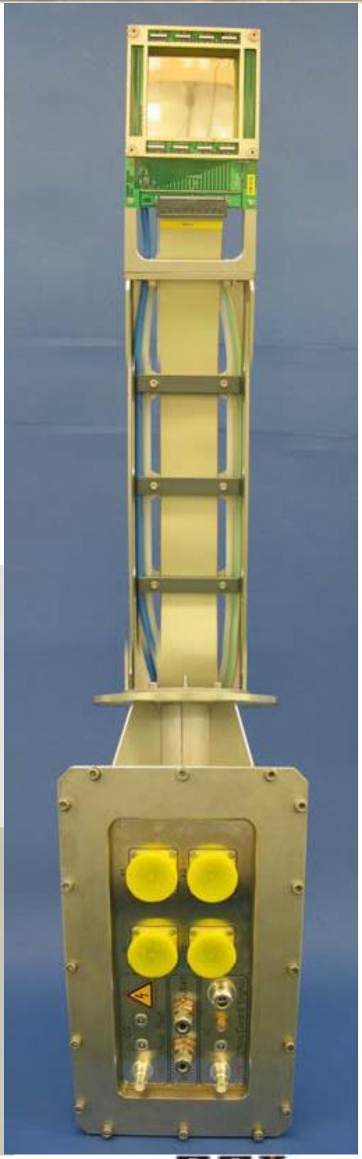

Outline:

- Scintillation screens:
  emission of light, universal usage, limited dynamic range
- SEM-Grid: emission of electrons, workhorse, limited resolution
  Multi Wire Proportional Chamber for slow extr. : gas ionization, limited resol.
- **Wire scanner:** emission of electrons, workhorse, scanning method
- Ionization Profile Monitor
- Optical Transition Radiation
- Synchrotron Light Monitors
- Summary

Idea: One wire is scanned through the beam!

Slow, linear scanner are used for:

- low energy protons
- high resolution measurements e.g. usable at e^+-e^- colliders
  by de-convolution $\sigma^2_{beam}=\sigma^2_{meas}-d^2_{wire}$
  $\Rightarrow$ resolution down to 10 µm range can be reached
- detection of beam halo.

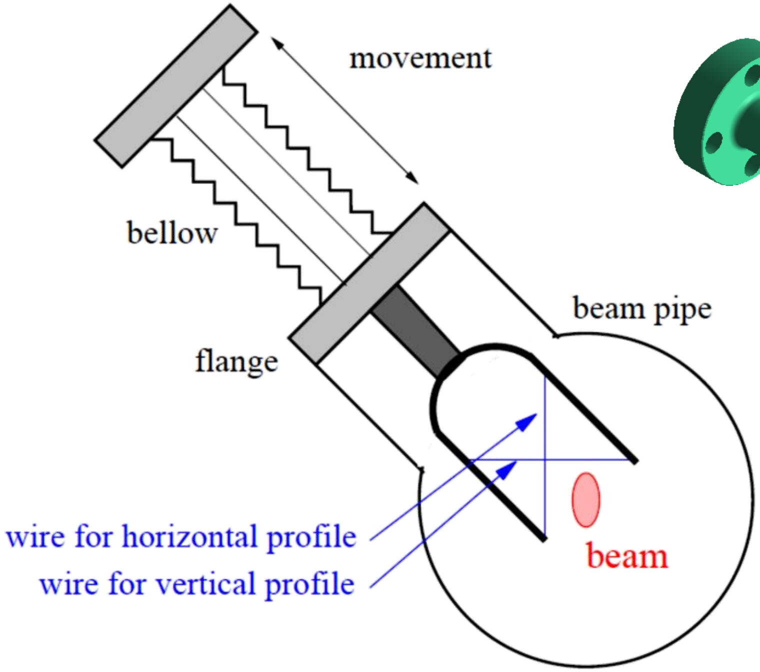

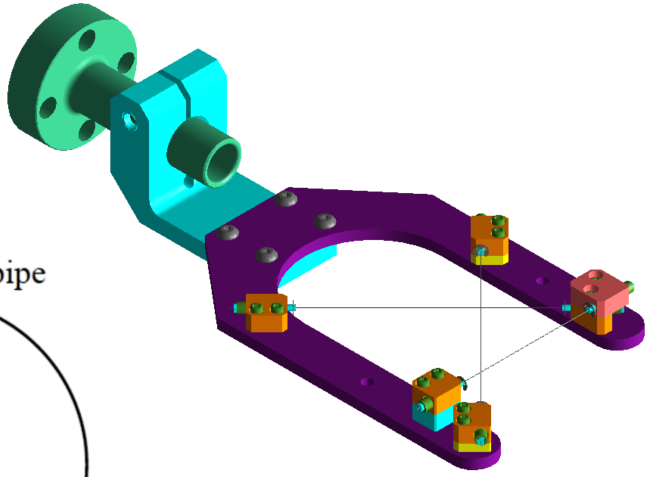

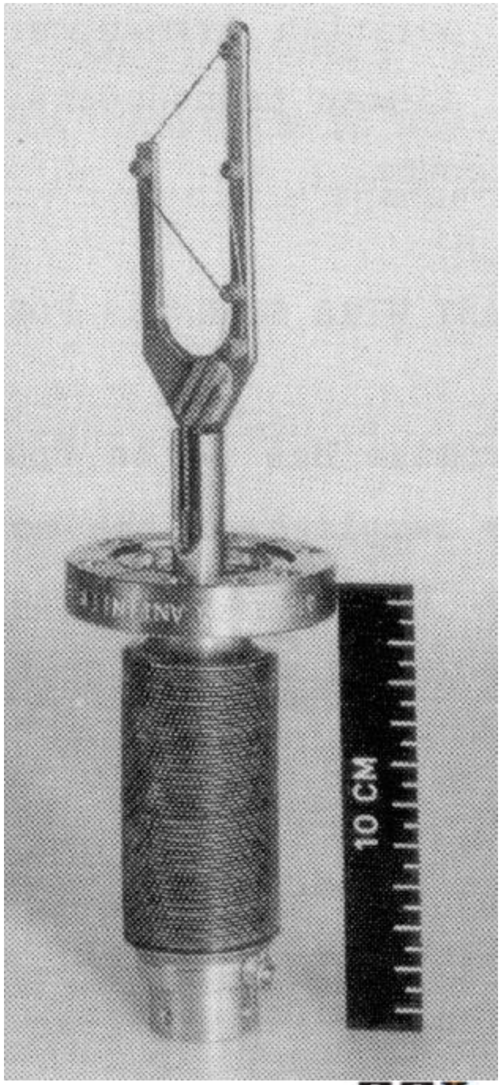

Slow, linear Wire Scanner

Idea: One wire is scanned through the beam!

Slow, linear scanner are used for:

- low energy protons
- high resolution measurements e.g. usable at e^+-e^- colliders
  by de-convolution $\sigma^2_{beam} = \sigma^2_{meas} - d^2_{wire}$
  $\Rightarrow$ resolution down to 10 μm range can be reached
- detection of beam halo.

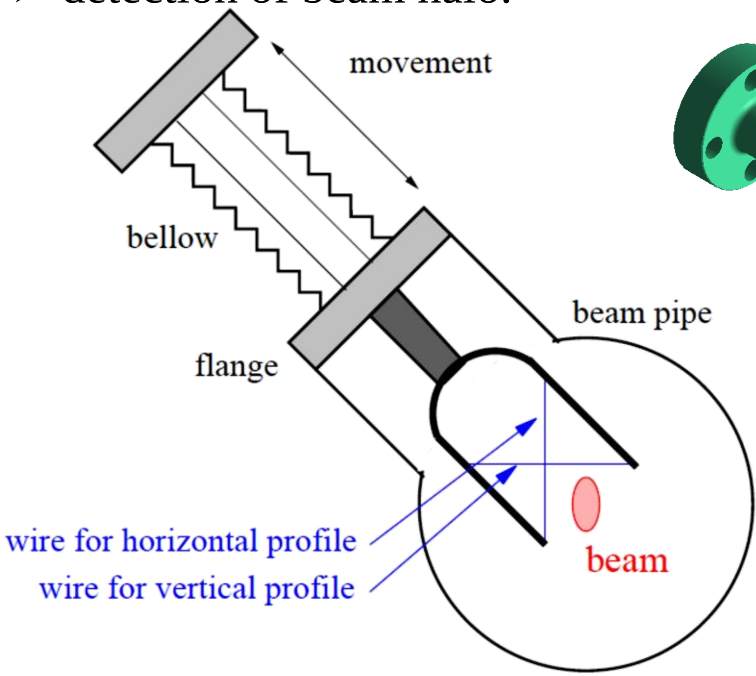

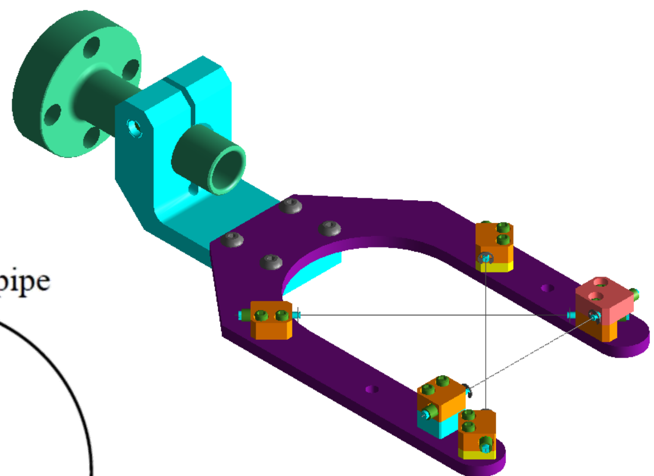

In a synchrotron ***one*** wire is scanned though the beam as fast as possible.

Fast pendulum scanner for synchrotrons; sometimes it is called ***'flying wire'***:

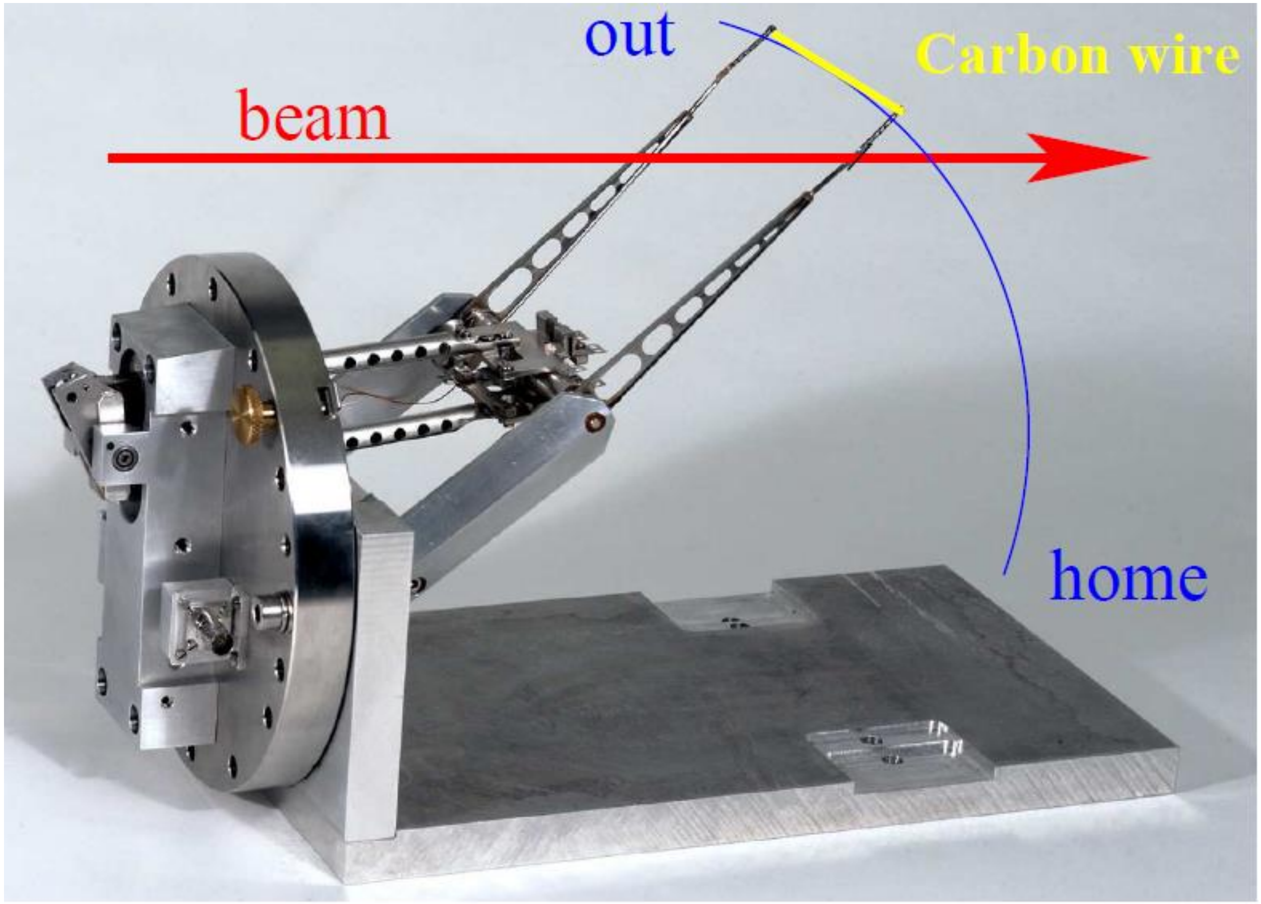

Usage of Wire Scanners

Material: carbon or SiC → low Z-material for low energy loss and high temperature.

Thickness: down to 10 μm → high resolution.

Detection: Either the **secondary current** (like SEM-grid) or
high energy **secondary particles** (like beam loss monitor)
flying wire: only sec. particle detection due to induced current by movement.

Secondary particles:

Proton beam → hadrons shower (π, n, p...)

Electron beam → Bremsstrahlung photons.

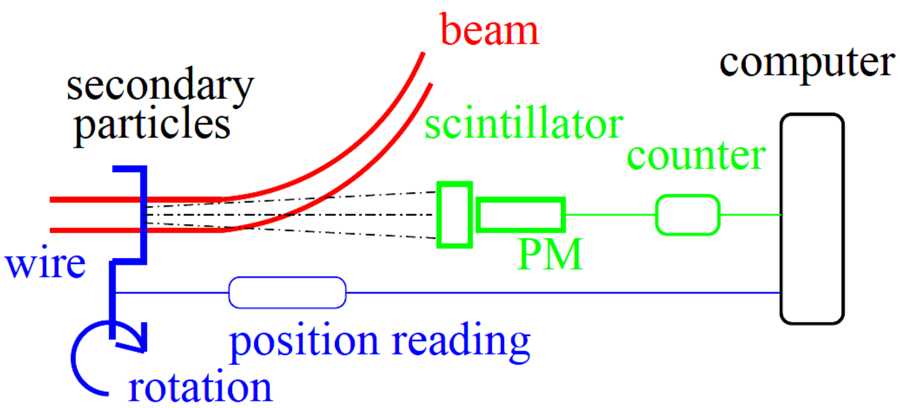

Proton impact on scanner at CERN-PS Booster:

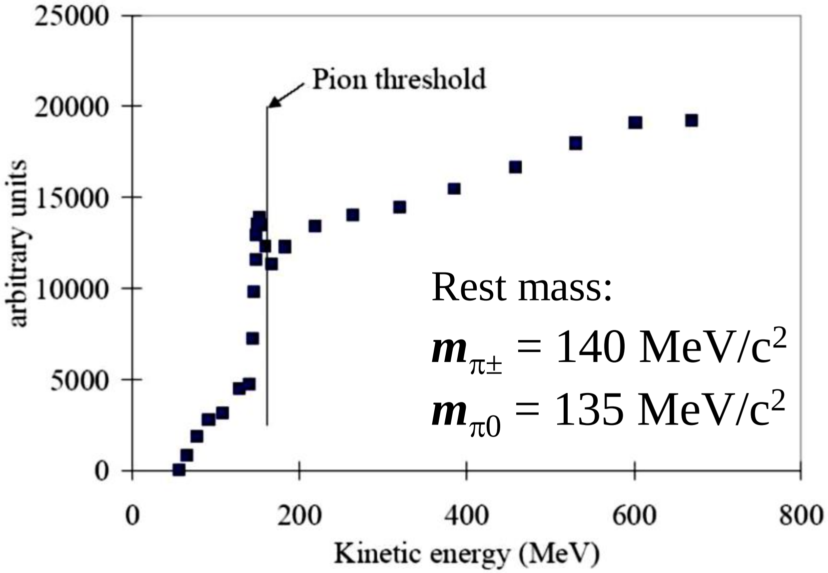

Kinematics of flying wire:

Velocity during passage typically 10 m/s = 36 km/h and typical beam size ∅ 10 mm

⇒ time for traversing the beam $t \approx 1$ ms

Comparison between SEM-Grid and Wire Scanners

Grid: Measurement at a single moment in time

Scanner: Fast variations can not be monitored

$\rightarrow$ for pulsed LINACs precise synchronization is needed

---

Grid: Not adequate at synchrotrons for stored beam parameters

Scanner: At high energy synchrotrons flying wire scanners are nearly non-destructive

---

Grid: Resolution of a grid is fixed by the wire distance (typically 1 mm)

Scanner: For slow scanners the resolution is about the wire thickness (down to 10 µm)

$\rightarrow$ used for e−-beams having small sizes (down to 10 µm)

Grid: Needs one electronics channel per wire

$\rightarrow$ expensive electronics and data acquisition

Scanner: Needs a precise movable feed-through $\rightarrow$ expensive mechanics.

Outline:

- Scintillation screens:
  emission of light, universal usage, limited dynamic range
- SEM-Grid: emission of electrons, workhorse, limited resolution
- Wire scanner: emission of electrons, workhorse, scanning method
  Multi Wire Proportional Chamber for slow extr. : gas ionization, limited resol.
- **Ionization Profile Monitor:**
  secondary particle detection from interaction beam-residual gas
- Optical Transition Radiation
- Synchrotron Light Monitors
- Summary

Non-destructive device for proton synchrotron:

- beam ionizes the residual gas by electronic stopping
- gas ions or e⁻ accelerated by E -field ≈1 kV/cm
- spatial resolved single particle detection

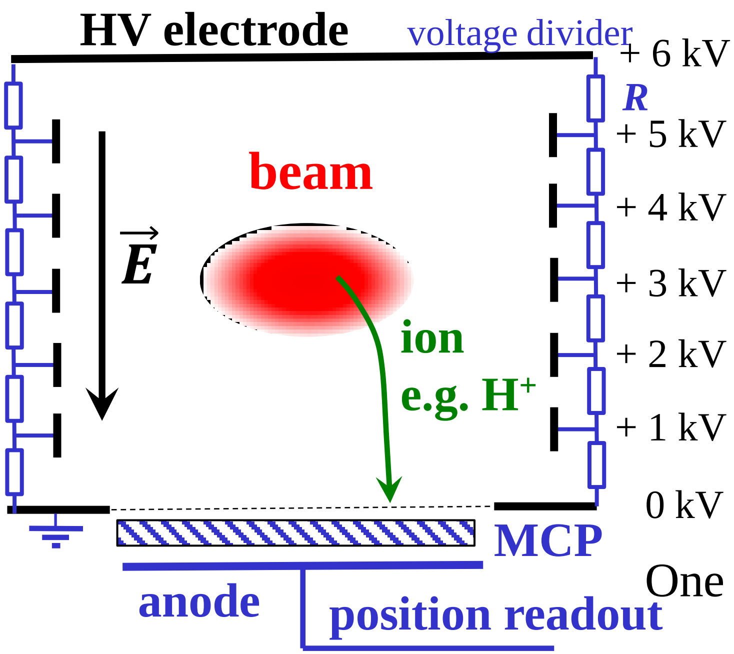

One device per plane

Realization at GSI synchrotron:

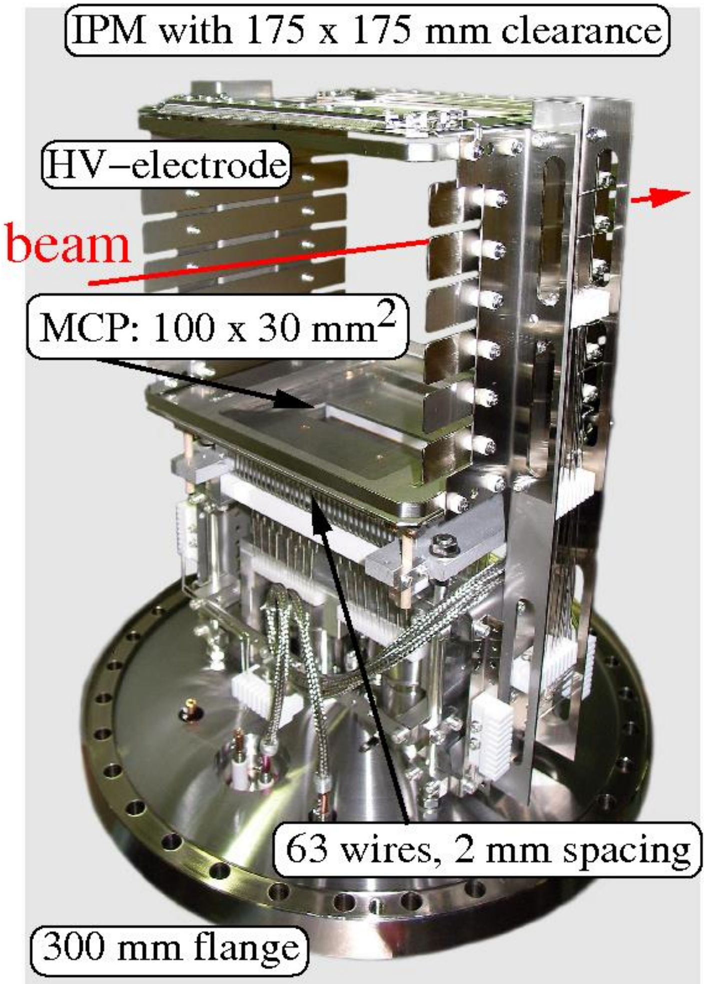

Typical vacuum pressure:

Transfer line: N_2 $10^{-8}...10^{-6}$ mbar $\cong 3\cdot10^8...3\cdot10^{10}$ cm^{-3}

Synchrotron: H_2 $10^{-11}...10^{-9}$ mbar $\cong 3\cdot10^5...3\cdot10^7$ cm^{-3}

The realization for the heavy ion storage ring ESR at GSI:

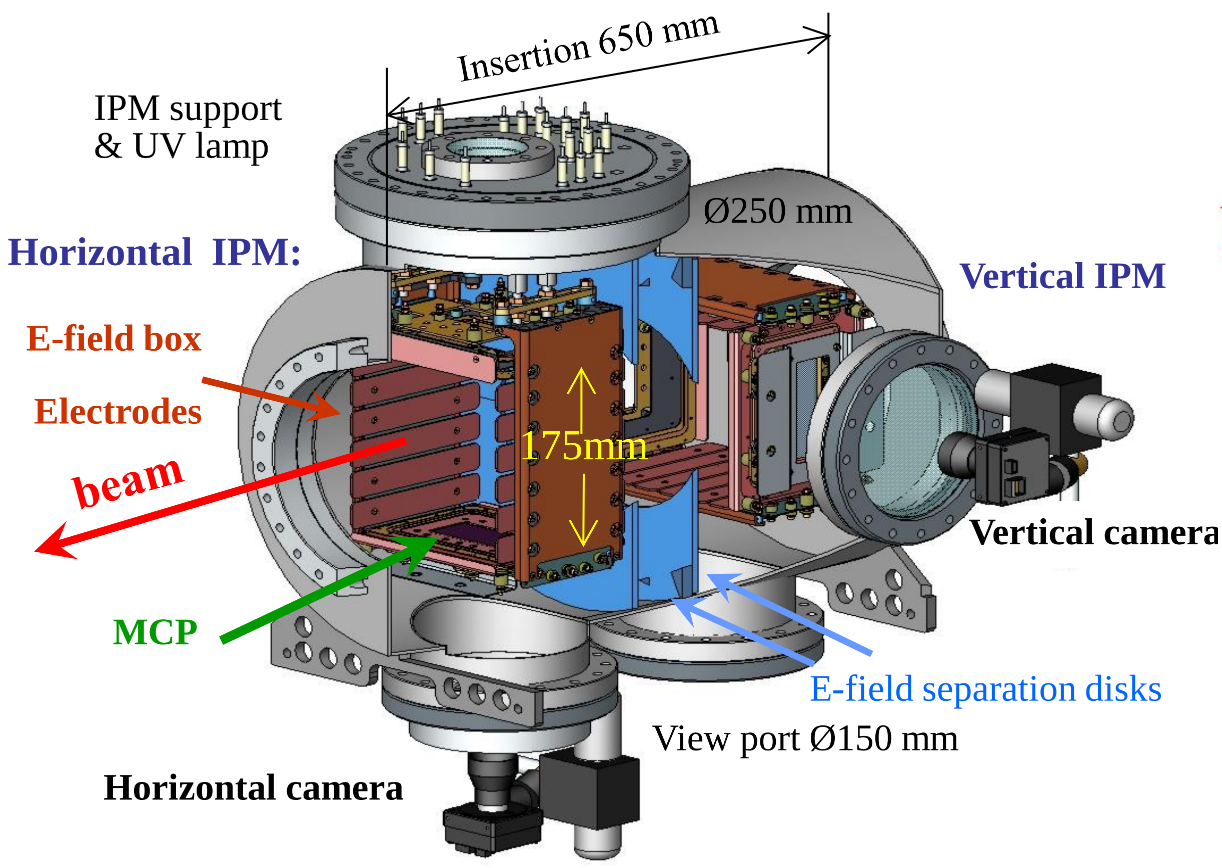

Realization at GSI synchrotron:

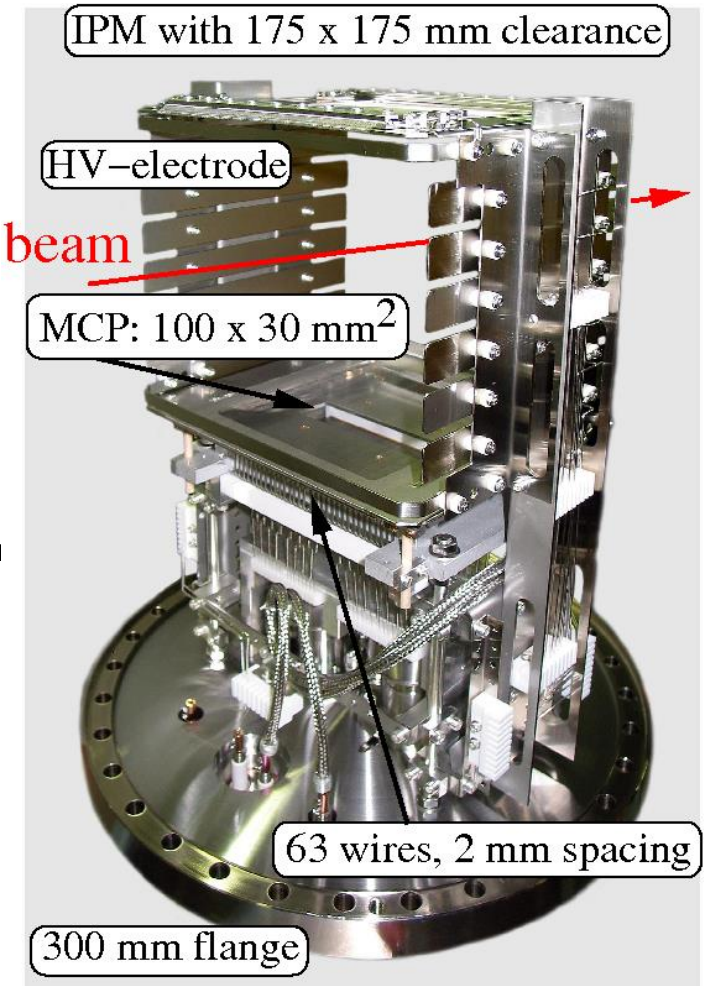

Ionization Profile Monitor Realization

The realization for the heavy ion storage ring ESR at GSI:

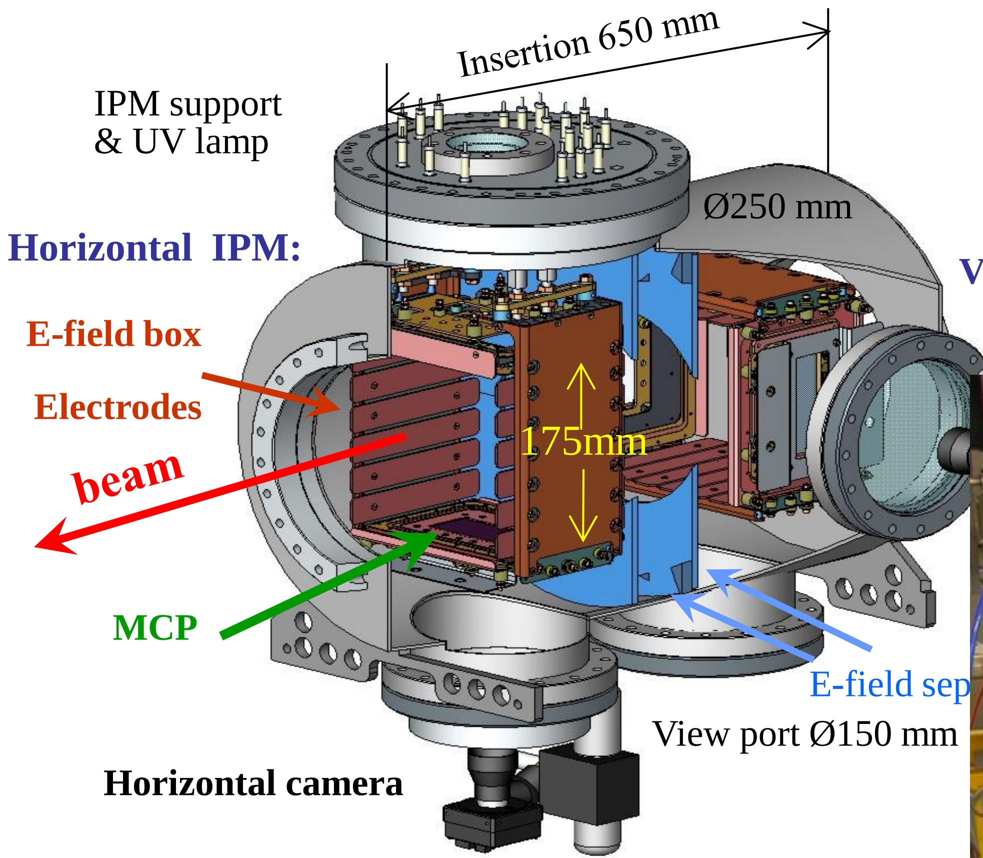

Realization at GSI synchrotron:

→ IPM measure

Alternative: e^- detection in an external magnetic field

$\rightarrow$ cyclotron radius $r_c = \sqrt{2m_e E_{kin,\perp}}/eB \;\Rightarrow\; r_c < 0.1\,\text{mm for } B = 0.1\,\text{T}$

$E_{kin,}$ given by atomic physics, 0.1 mm is internal resolution of MCP.

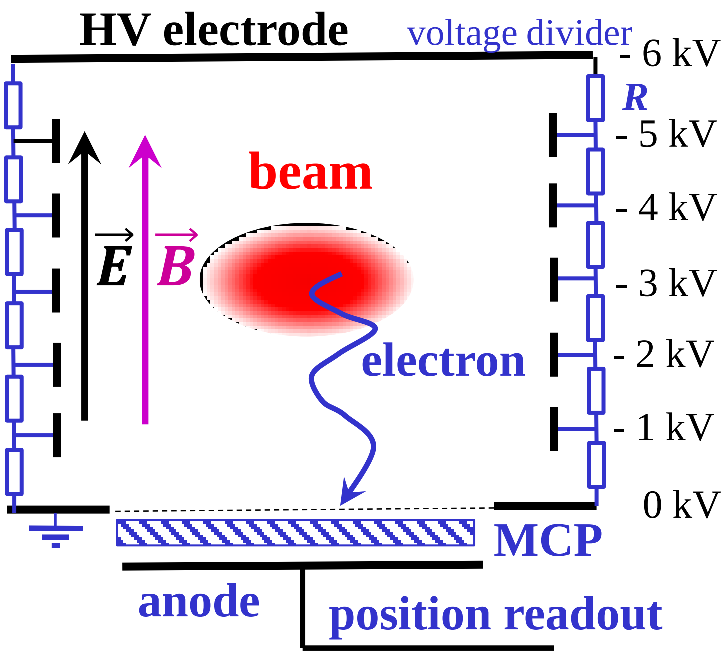

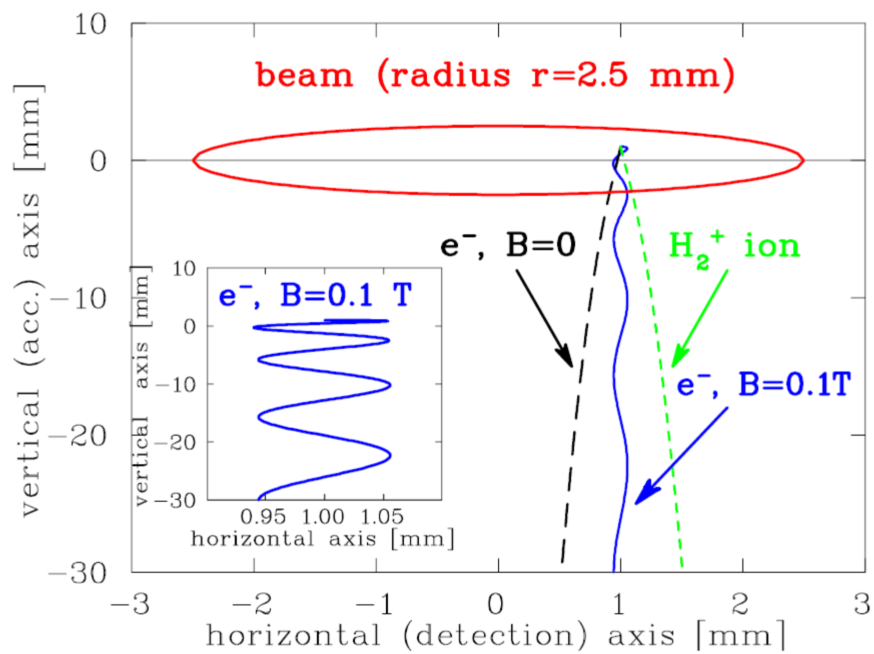

Time-of-flight: ≈1 ns → 2 or 3 cycles.

B-field: By dipole magnets with large aperture → IPM is expensive device.

Magnetic field for electron guidance:

Maximum image distortion:

5% of beam width ⇒ $\Delta B/B$ < 1 %

Challenges:

- High ***B***-field homogeneity of 1 %
- Clearance up to 500 mm
- Correctors required
  to compensate beam steering
- Insertion length 2.5 m incl. correctors

For MCP wire-array readout
lower clearance required

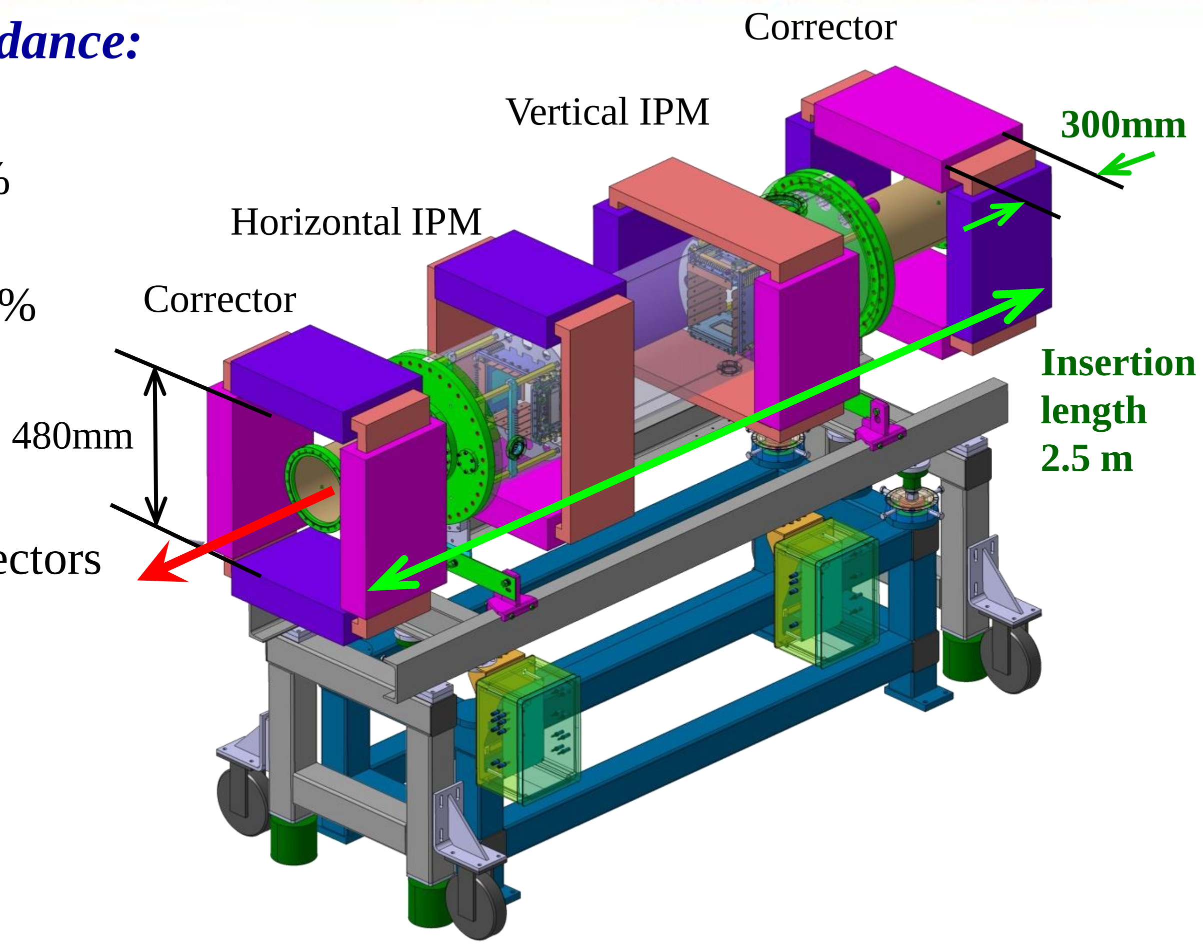

IPM: Magnet Design

Magnetic field for electron guidance:

Maximum image distortion:

5% of beam width ⇒ $\Delta B/B < 1\,\%$

Challenges:

- High ***B***-field homogeneity of 1 %
- Clearance up to 500 mm
- Correctors required
  to compensate beam steering
- Insertion length 2.5 m incl. correctors

For MCP wire-array readout
lower clearance required

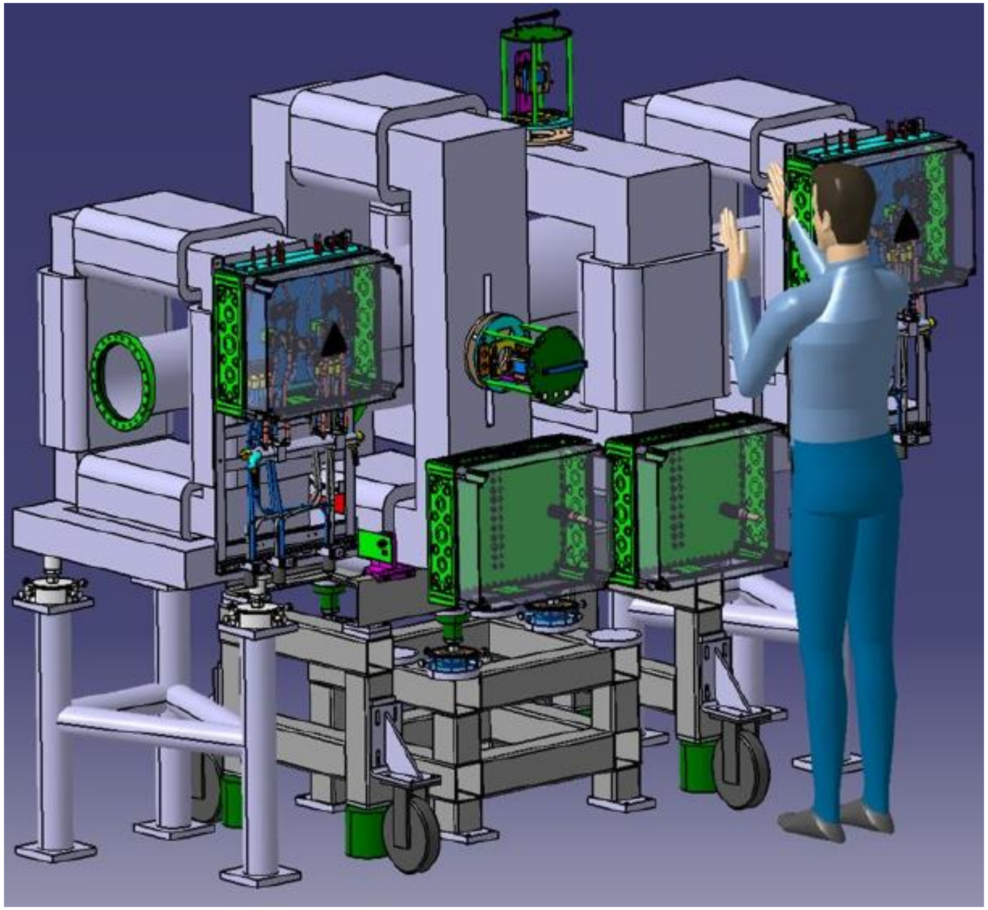

'Adiabatic' Damping during Acceleration

The emittance $\varepsilon = \int dxdx'$ is defined via the position deviation and angle in **lab-frame**

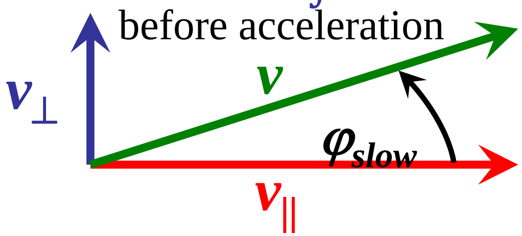

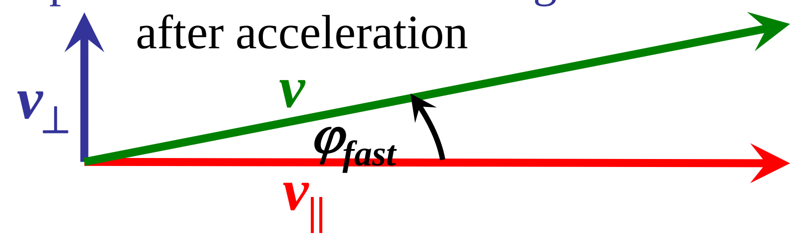

After acceleration the longitudinal velocity is increased $\Rightarrow$ angle φ is smaller

The angle is expressed in momenta: $x' = p_\perp / p_\parallel$ the emittance is $\langle xx' \rangle = 0$: $\varepsilon = x \cdot x' = x \cdot p_\perp / p_\parallel$

$\Rightarrow$ under ideal conditions the emittance can be normalized to the momentum $p_\parallel = \gamma \cdot m \cdot \beta c$

$\Rightarrow$ normalized emittance $\varepsilon_{norm} = \beta\gamma \cdot \varepsilon$ is preserved with the Lorentz factor γ and velocity $\beta = v/c$

Example: Acceleration in GSI-synchrotron for C^{6+} from 6.7 → 600 MeV/u (β = 12 → 79 %) observed by IPM

theoretical width: $\langle x \rangle_f = \sqrt{\frac{\beta_i \cdot \gamma_i}{\beta_f \cdot \gamma_f}} \cdot \langle x \rangle_i$

$= 0.33 \cdot \langle x \rangle_i$

measured width: $\langle x \rangle_f \approx 0.37 \cdot \langle x \rangle_i$

IPM is well suited
for long time observations
without beam disturbance
→ mainly used at proton synchrotrons.

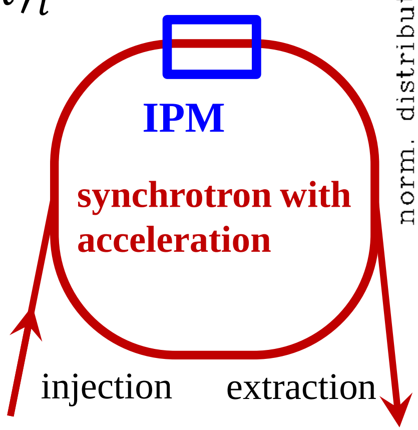

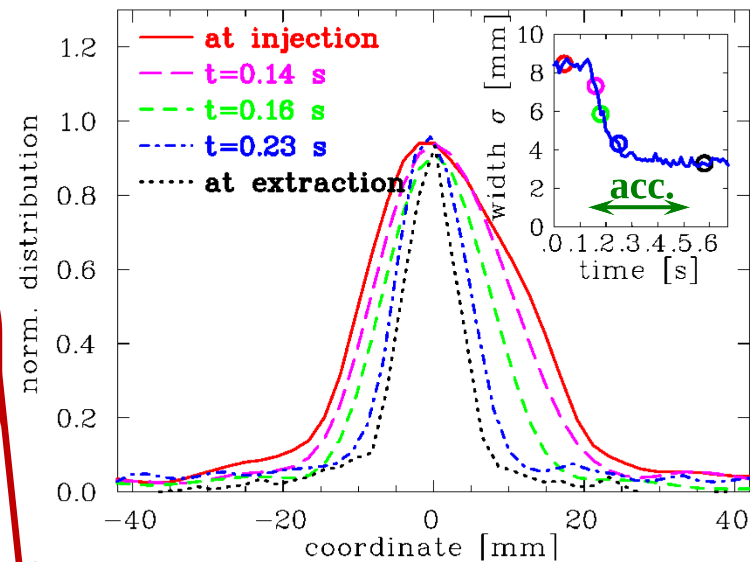

Emittance 'Control' via Chopped Injection

For a multi-turn injection the emittance can be controlled by beam chopping

Bumper magnet action:

- First beamlet injected on central path
- Successive filling of 'outer' phase space

⇒ stored horizontal emittance varies

⇒ vertical emittance un-changed

⇒ injected current increase for longer t_{chop}

Monitoring by IPM

Example: C^{6+} at 6.7 MeV/u, up to $6{\cdot}10^9$ ions per fill with multi-turn injection at GSI synchrotron, 5μs/turn

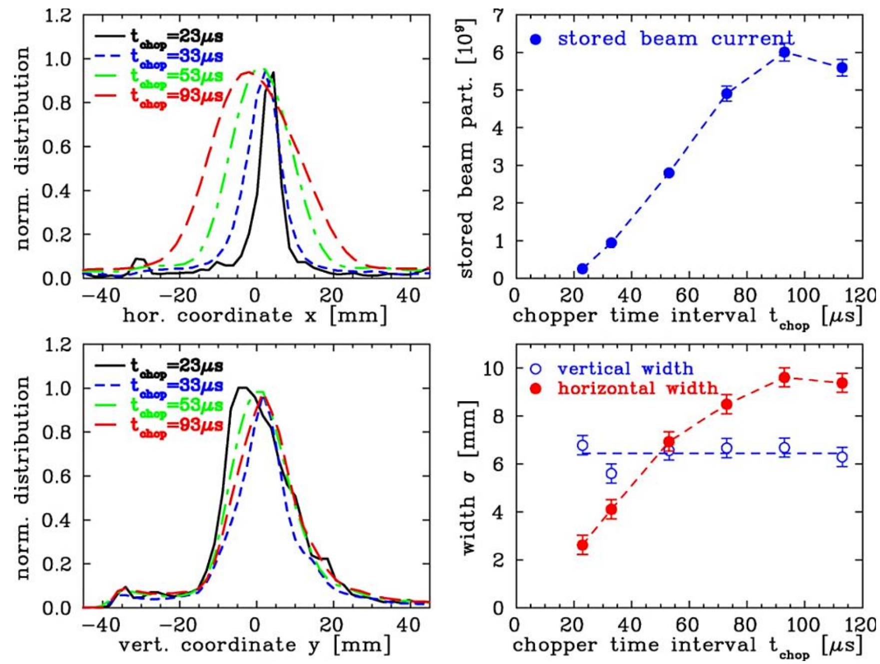

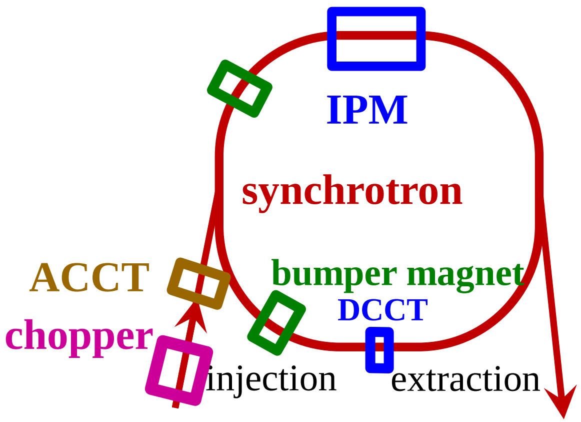

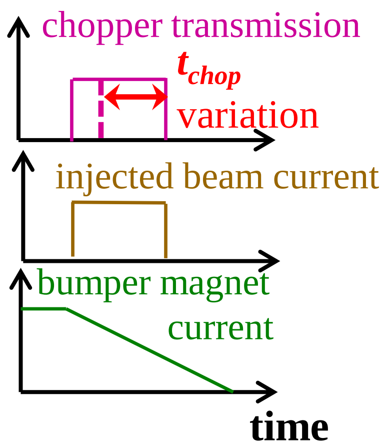

Emittance Enlargement by Injection Mis-steering

Emittance conservation requires precise injection matching

Wrong angle of injected beam:

- injection into outer phase space → large *β*-amplitude i.e. large beam
- might result in 'hollow' beam
- filling of acceptance i.e. loss of particles

⇒ Hadron beams: larger emittance after acceleration

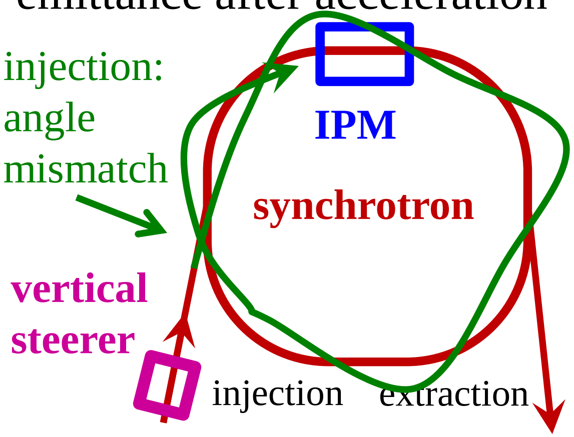

Example: Variation of vertical injection angle by magnetic steerer
Beam: C^{6+} at 6.7 MeV/u acc. to 600 MeV/u, up to $6\cdot10^9$ ions per fill with multi-turn injection, IPM integration 0.5 ms i.e. ≈ 100 turns

Vertical profile **at** injection:

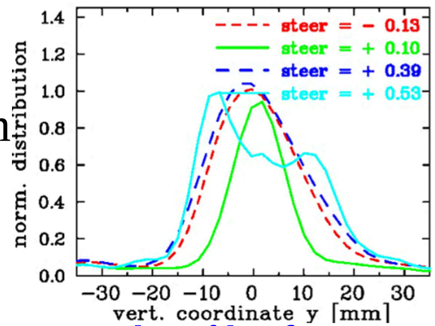

Horizontal profile **at** injection:

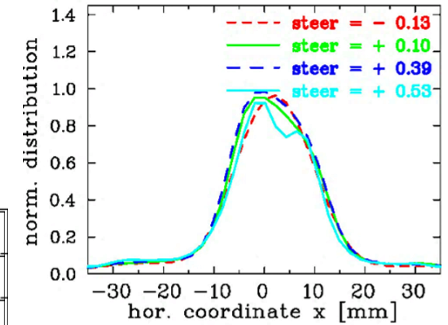

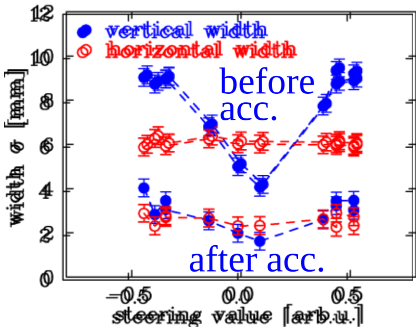

Vertical profile **after** acc.:

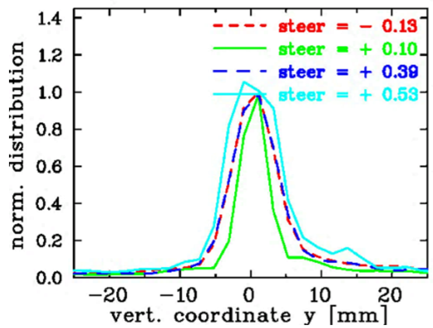

Horizontal profile **after** acc.:

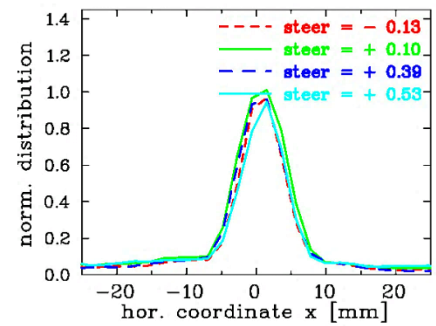

Schematic simulation:
Courtesy M. Syphers

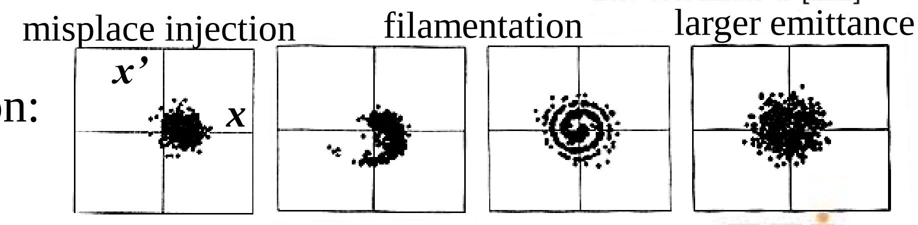

Ideal case of injection matching:

Orientation of injected beam matches phase space as given by synchrotron

Twiss parameters α, β, and γ i.e. 'machine emittance'

⇔ no change after each turn ⇔ stable storage

⇔ The beam ellipse $\boldsymbol{\sigma}_{beam}$ correspond to the machine ellipse at injection point for N=0 i.e.

$$\boldsymbol{\sigma}_{beam}(N=0) = \varepsilon_{beam}\begin{pmatrix}\beta_{synch} & -\alpha_{synch}\\ -\alpha_{synch} & \gamma_{synch}\end{pmatrix}$$

⇒ **only in this case stable storage** (math: $t \rightarrow \infty$)

$$\boldsymbol{\sigma}_{beam}(N=0) = \boldsymbol{\sigma}_{beam}(N \rightarrow \infty)$$

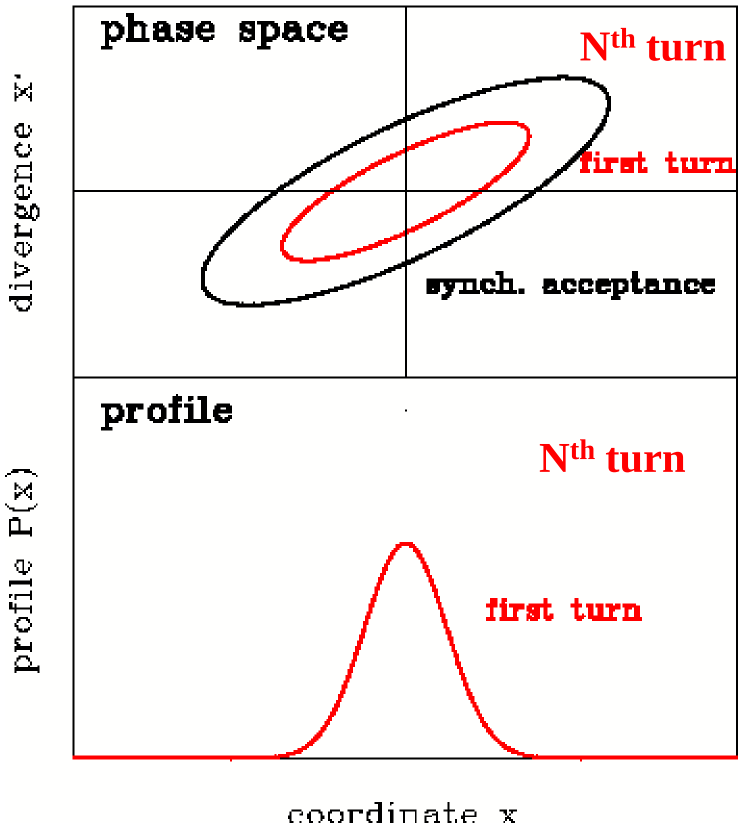

Injection Matching into a Synchrotron: Phase Space Mismatch

Ideal case of injection matching:
Orientation of injected beam matches
phase space as given by synchrotron
Twiss parameters α, β, and γ i.e. 'machine emittance'
⇔ no change after each turn ⇔ stable storage

Mis-matched case:

- The beam ellipse $\boldsymbol{\sigma}_{beam}$ has different orientation as machine ellipse at injection point for N=0 i.e.
- Transformation after one turn

$$\boldsymbol{\sigma}_{beam}(N=1) = \mathbf{M}\boldsymbol{\sigma}_{beam}(N=0)\,\mathbf{M}^T \neq \boldsymbol{\sigma}_{beam}(N=0)$$

i.e. rotation in phase space by the tune
i.e. phase advance per turn
Depictive argument: Always particle on both ellipse

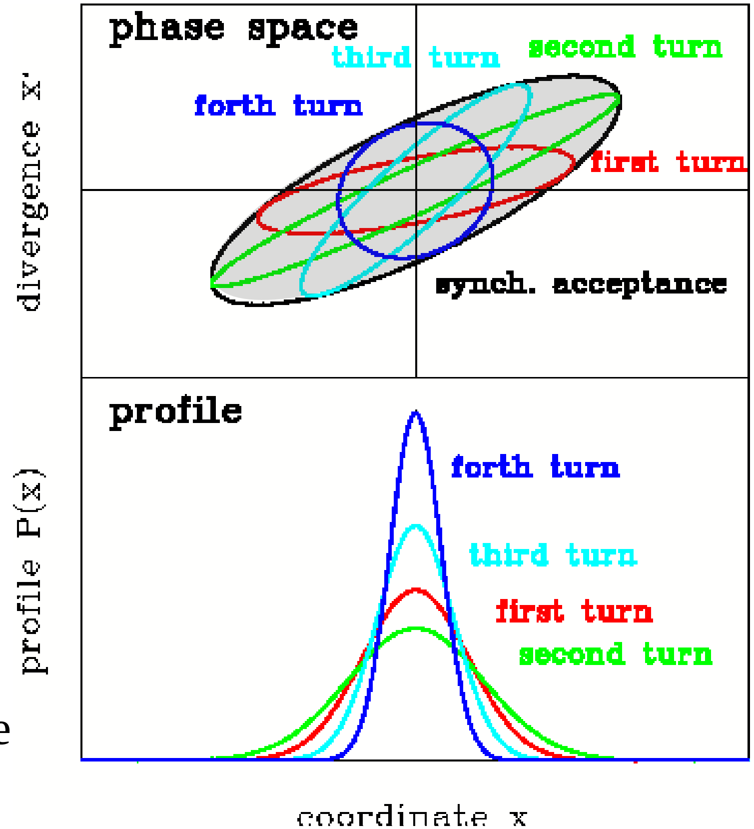

Observable quantity: Beam profile oscillates

After many turns:

Particle have different tunes e.g. by longitudinal momentum deviation and chromaticity $\frac{\Delta Q}{Q_0} = \xi \cdot \frac{\Delta p}{p_0}$

or space charge ΔQ_{incoh} ⇒ Entire transverse phase space is filled i.e. beam with enlarged emittance

Mis-matched injection into a synchrotron:

Can be monitored by beam profile measurement:

Example: Injection of a 80 ns bunch of protons into CERN PS at 1.4 GeV/u (2.2 μs revolution time)

Profile measurement by SEM-Grid

- Turn-by-turn profile variation related to tune
- Used for improvement of injection parameters

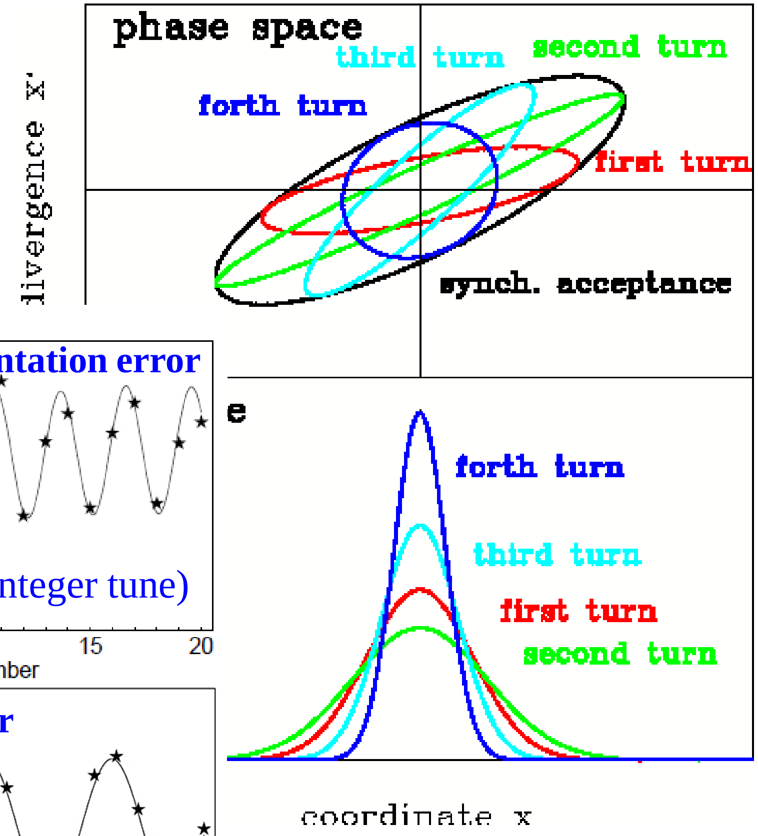

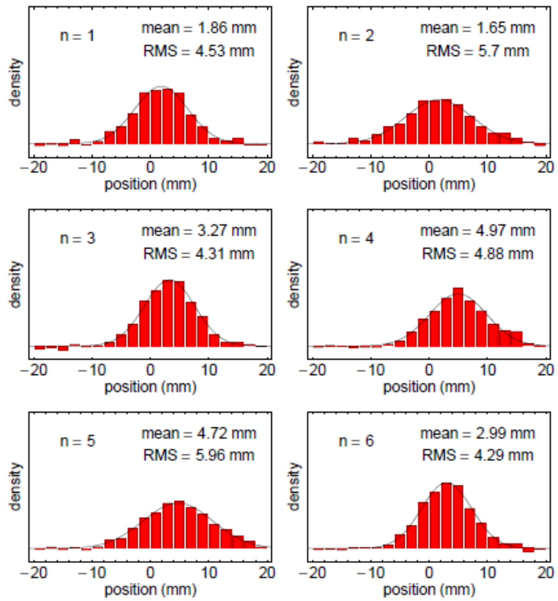

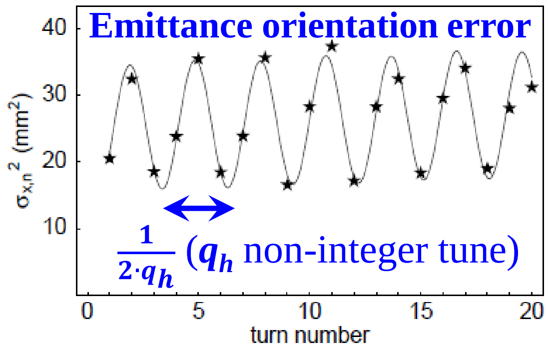

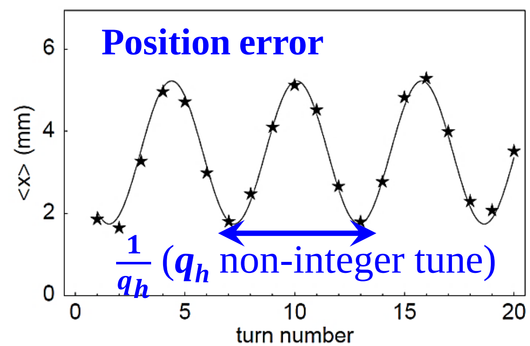

From M. Benedikt et al., DIPAC 2001

Outline:

- Scintillation screens:
  emission of light. universal usage, limited dynamic range
- SEM-Grid: emission of electrons, workhorse, limited resolution
- Wire scanner: emission of electrons, workhorse, scanning method
  Multi Wire Proportional Chamber for slow extr. : gas ionization, limited resol.
-
- Ionization Profile Monitor:
  secondary particle detection from interaction beam-residual gas
- **Optical Transition Radiation:**
  crossing material boundary, for relativistic beams only
- Synchrotron Light Monitors
- Summary

Optical Transition Radiation OTR for a single charge *e*:

Assuming a charge ***e*** approaches an ideal conducting boundary e.g. metal foil

- image charge is created by electric field
- dipole type field pattern
- field distribution depends on velocity β and Lorentz factor γ due to relativistic trans. field increase
- penetration of charge through surface within t < 10 fs: sudden change of source distribution
- emission of radiation with dipole characteristic

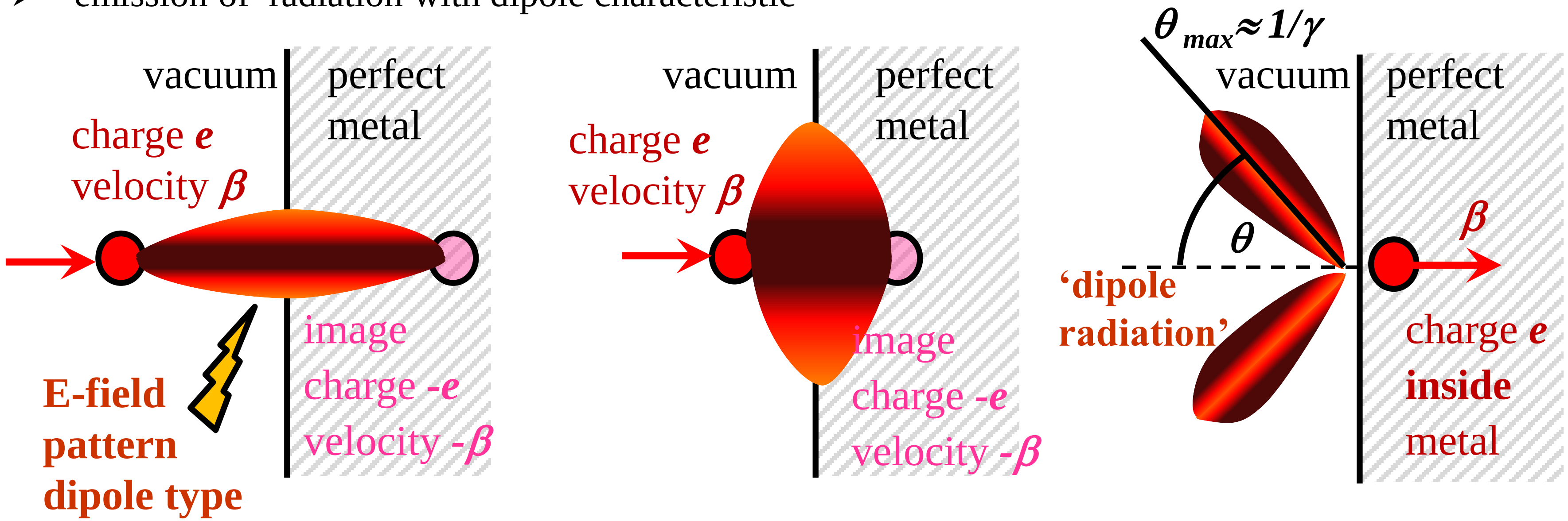

sudden change charge distribution
rearrangement of sources ⇔ radiation

Other physical interpretation: Impedance mismatch at boundary leads to radiation

Optical Transition Radiation OTR can be described in classical physics:

approximated formula for normal incidence & in-plane polarization:

$$\frac{d^2W}{d\theta\, d\omega} \approx \frac{2e^2\beta^2}{\pi c} \cdot \frac{\sin^2\theta \cdot \cos^2\theta}{\left(1-\beta^2\cos^2\theta\right)^2}$$

W: radiated energy

ω: frequency of wave

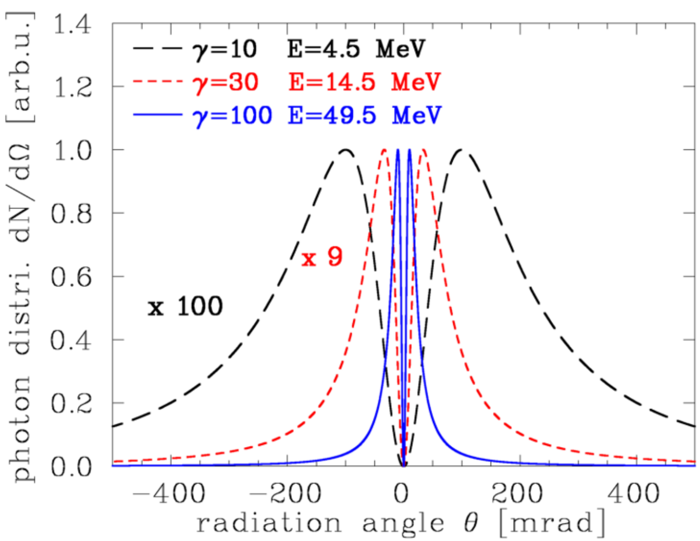

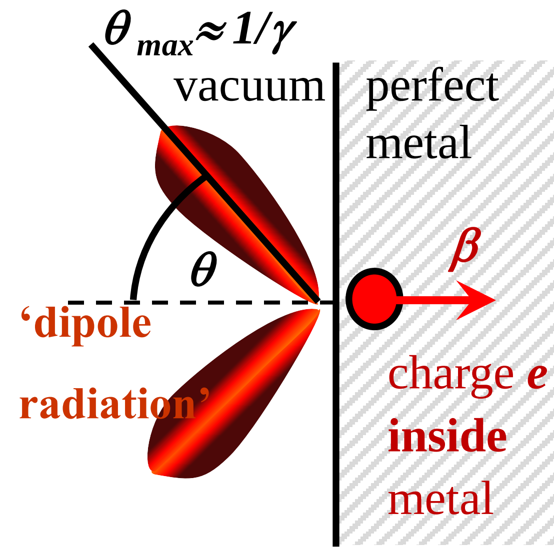

Angular distribution of radiation in optical spectrum:

- lope emission pattern depends on velocity or Lorentz factor γ
- peak at angle $\theta \approx 1/\gamma$
- emitted energy i.e. amount of photons scales with $W \propto \beta^2$
- broad wave length spectrum (i.e. no dependence on ω)

→ suited for high energy electrons

sudden change charge distribution
rearrangement of sources ⇔ radiation

OTR with 45^0 beam incidence and observation at 90^0 :

approximated formula for 45^0 incidence& in plane polarization:

$$\frac{d^2W}{d\theta\, d\omega} \approx \frac{2e^2\beta^2}{\pi c} \cdot \left(\frac{\sin\theta}{1-\beta\cos\theta} + \frac{\cos\theta}{1-\beta\sin\theta} \right)^2$$

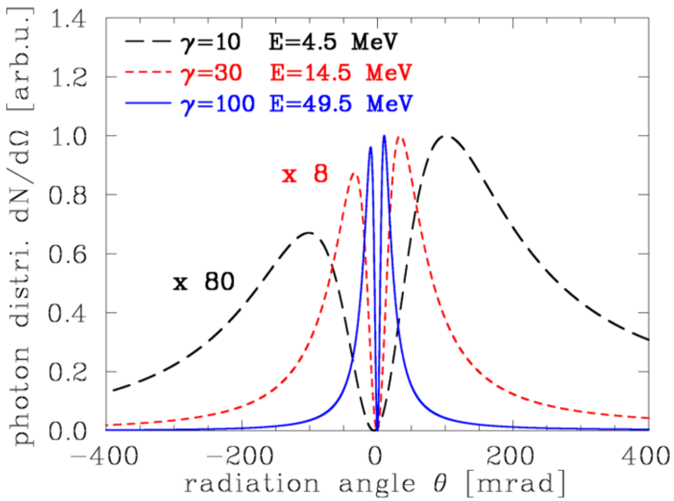

Angular distribution of radiation in optical spectrum:

- emission pattern depends on velocity
- peak at angle $\theta \approx 1/\gamma$
- emitted energy scales with $W \propto \beta^2$
- symmetric with respect to θ for $\gamma > 100$

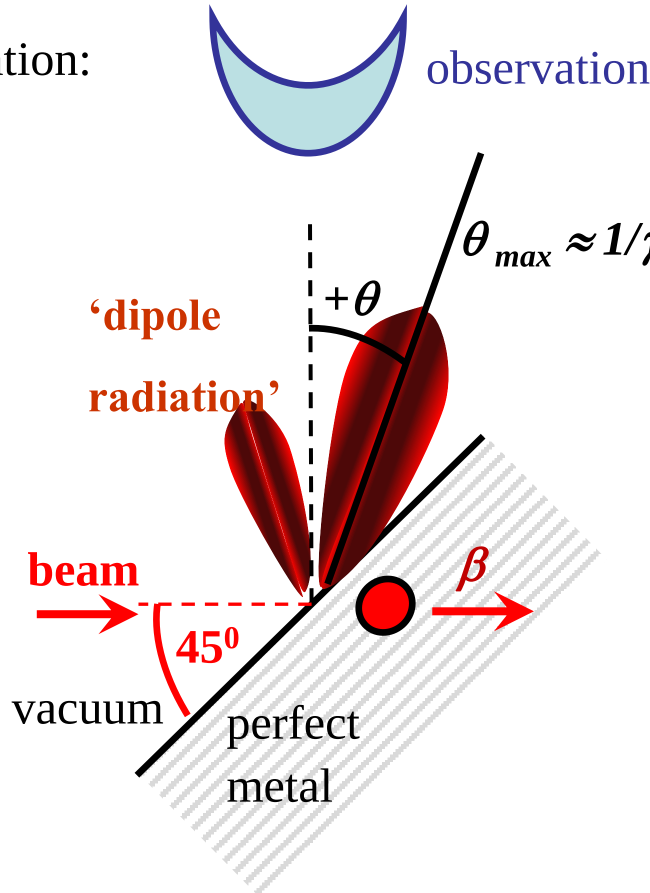

Remark: polarization of emitted light:

- in scattering plane → parallel E-vector
- perpendicular plane → rectangular E-vector

OTR is emitted by charged particle passage through a material boundary.

Photon distribution:
within a solid angle $d\Omega$ and
Wavelength interval λ_{begin} to λ_{end}

$$\frac{dN_{photon}}{d\Omega} = N_{beam} \cdot \frac{2e^2\beta^2}{\pi c} \cdot \log\left(\frac{\lambda_{begin}}{\lambda_{end}}\right) \cdot \frac{\theta^2}{\left(\gamma^{-2}+\theta^2\right)^2}$$

- Detection: Optical 400 nm < λ < 800 nm

  using image intensified CCD

- Larger signal for relativistic beam $\gamma >> 1$
- Low divergence for $\gamma >> 1 \Rightarrow$ large signal

$\Rightarrow$ **well suited for e⁻ beams**

$\Rightarrow$ **p-beam only for E_{kin} > 10 GeV $\Leftrightarrow \gamma > 10$**

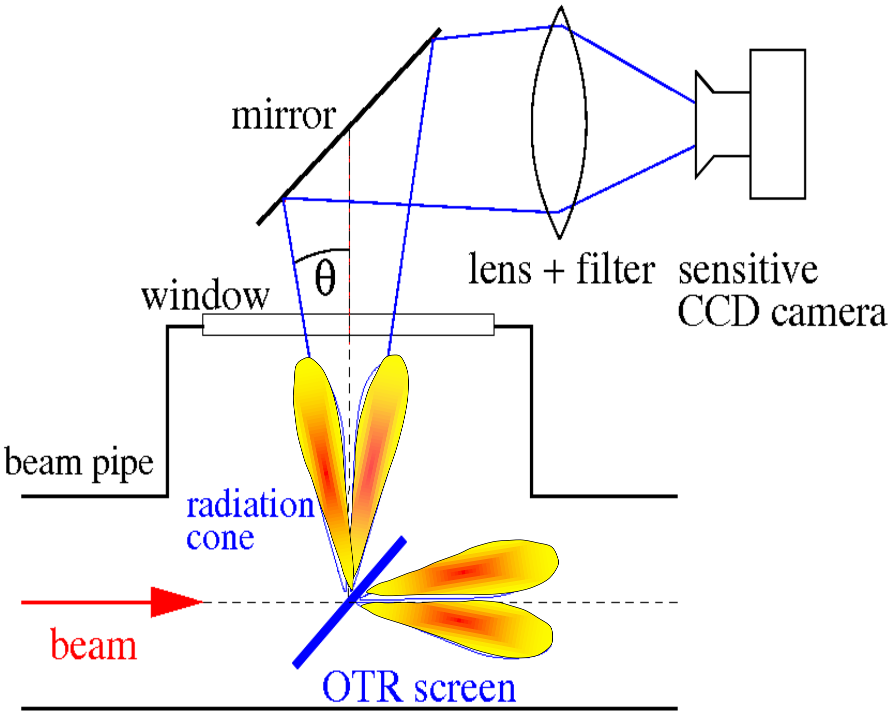

- Insertion of thin Al-foil under 45°
- Observation of low light by CCD.

Example of realization at TERATRON:

- Insertion of foil
  e.g. 5 μm Kapton coated with 0.1μm Al

Advantage: thin foil ⇒ low heating & straggling
2-dim image visible

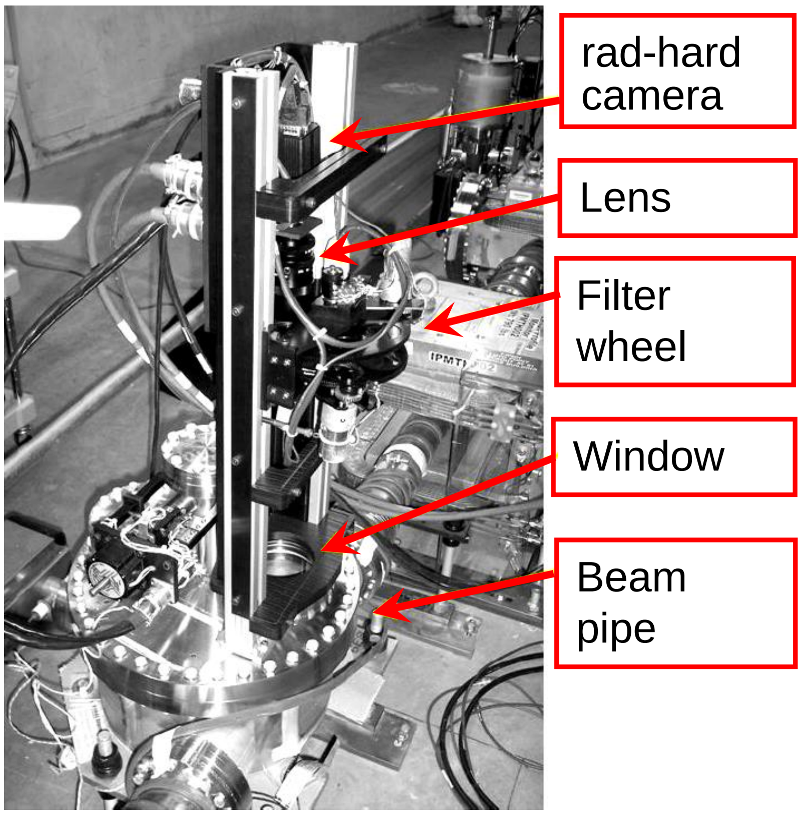

Results at FNAL-TEVATRON synchrotron with 150 GeV proton
Using fast camera: Turn-by-turn measurement

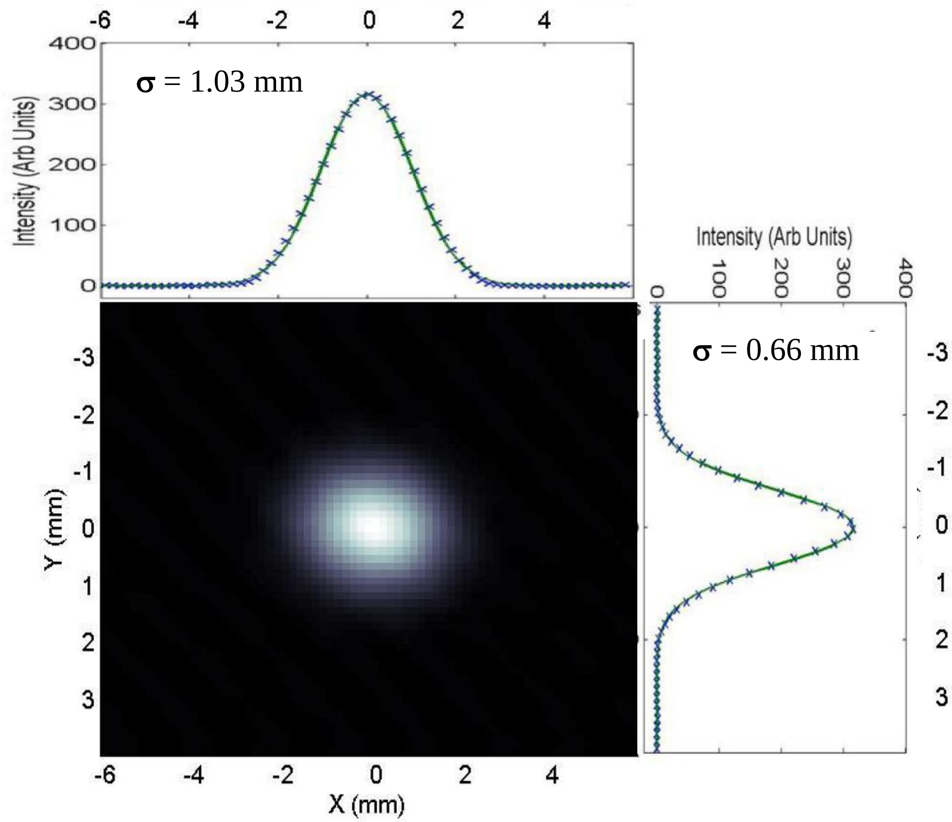

Courtesy V.E. Scarpine (FNAL) et al., BIW'06

OTR-Monitor: Prove of Radiation Hardness

Application:

Permanent observation of bam profile
direct in front of a target

Advantage of OTR:

- Thin foil i.e. low straggling and nuclear reactions
- Higher radiation hardness as scintillation screens
- 2-dim image as compared o 2 x 1-dim for SEM-Grid

***Example* for target diagnostics at FNAL:**

Insertion of OTR in front of NuMI target
120-150 GeV protons for neutrino physics
Online profile observation possible
OTR foil: 120 nm Aluminum on 6 μm Kapton

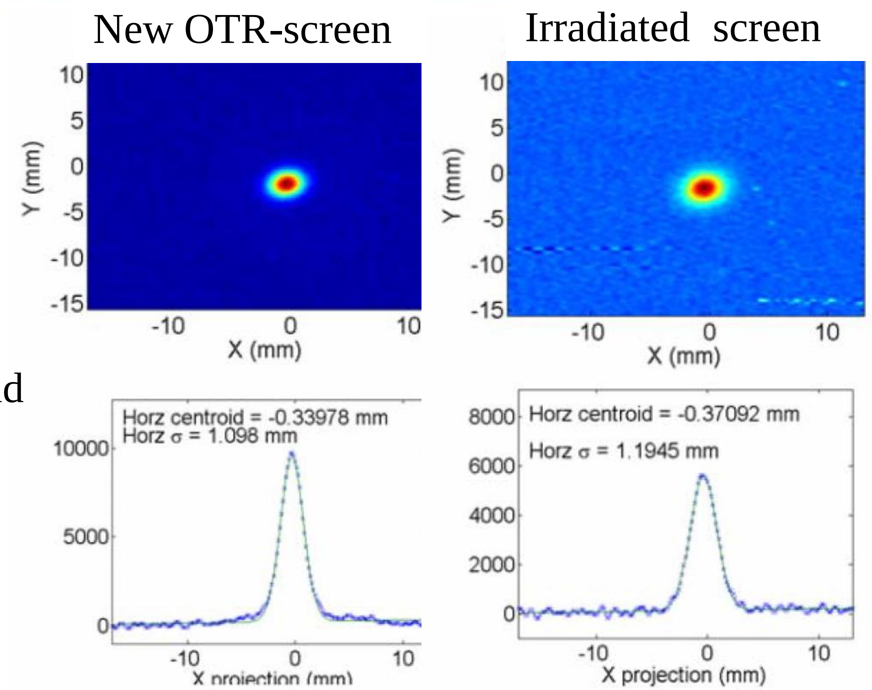

Radiation hardness test at FNAL:

$7 \cdot 10^{19}$ protons with 120 GeV in 70 days
→ half signal strength but ***same*** width reading

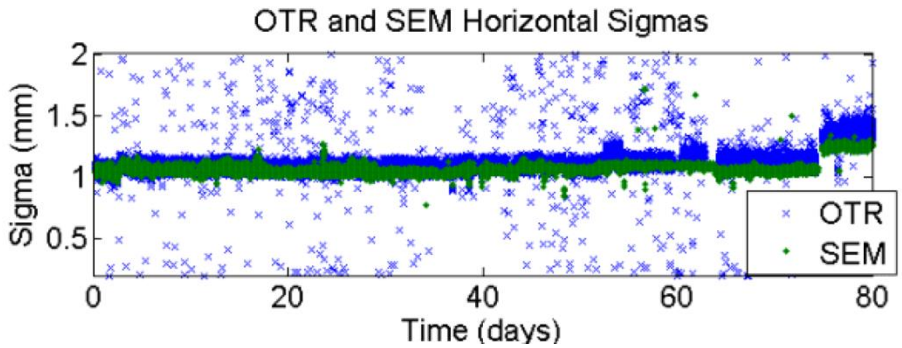

Courtesy V.E. Scarpine (FNAL) et al., PAC’07

Installation of OTR and scintillation screens on same drive :

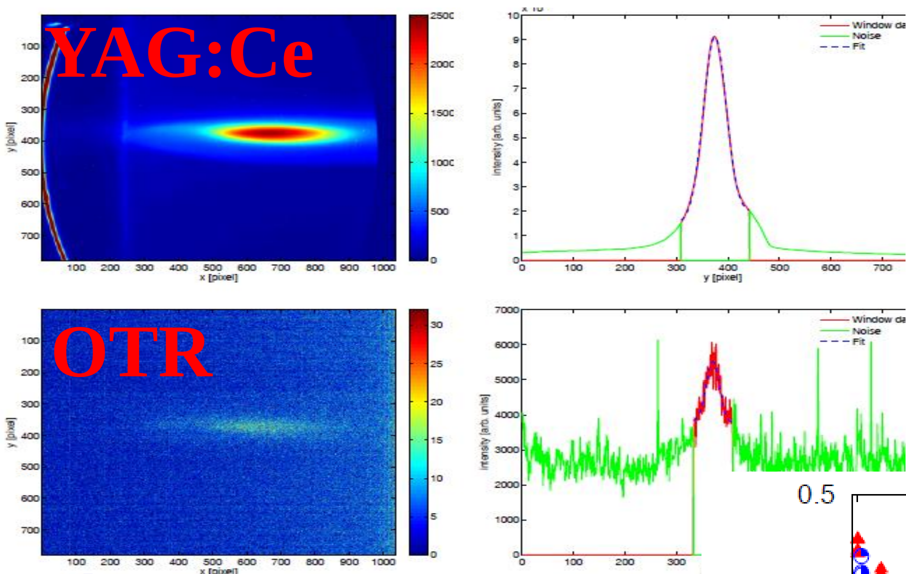

Example: ALBA LINAC 100 MeV

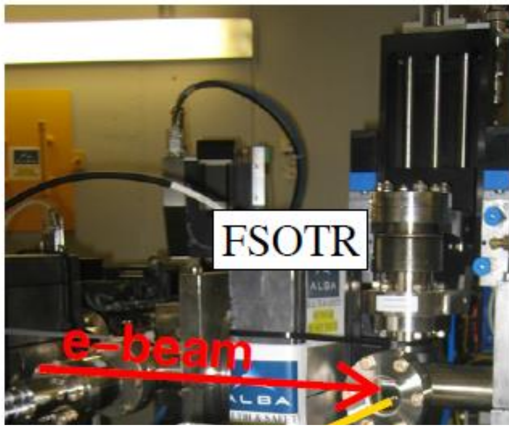

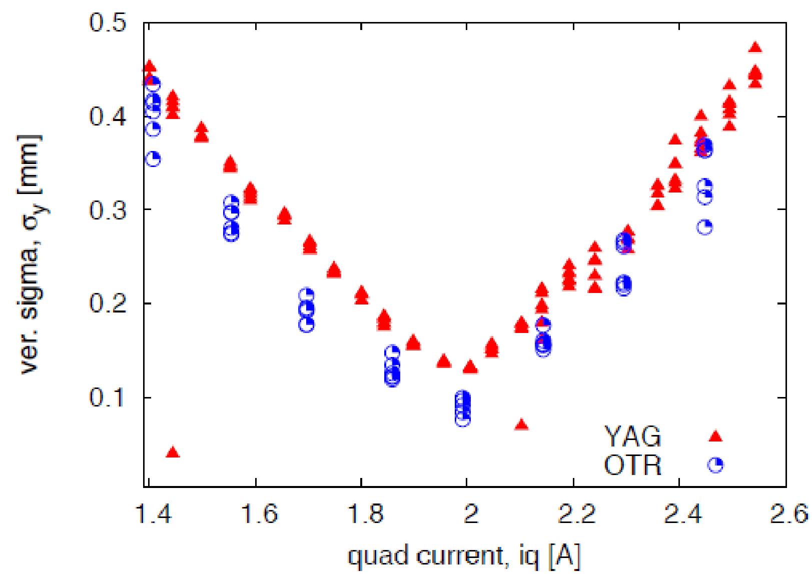

Results:

- Much more light from YAG:Ce for 100 MeV (γ=200) electrons light output $I_{YAG} \approx 10^5 I_{OTR}$
- Broader image from YAG:Ce due to finite shoulders or CCD saturation(?)

Courtesy of U. Iriso et al., DIPAC'09

Comparison between Scintillation Screens and OTR

OTR: electrodynamic process → beam intensity linear to # photons, high radiation hardness
Scint. Screen: complex atomic process → saturation possible, for some low radiation hardness

---

OTR: thin foil Al or Al on Mylar, down to 0.25 μm thickness
→ minimization of beam scattering (Al is low Z-material)
Scint. Screen: thickness ≈ 1 mm inorganic, fragile material, not radiation hard

---

OTR: low number of photons → expensive image intensified CCD
Scint. Screen: large number of photons → simple CCD sufficient

---

OTR: complex angular photon distribution → resolution limited
Scint. Screen: isotropic photon distribution → simple interpretation

---

OTR: large γ needed → e^--beam with E_{kin} > 100 MeV, proton-beam with E_{kin} > 100 GeV
Scint. Screen: for all beams

Remark: OTR **not** suited for LINAC-FEL due to **coherent** light emission (not covered here)
but scintilation screens can be used.

Outline:

- Scintillation screens:
  emission of light, universal usage, limited dynamic range
- SEM-Grid: emission of electrons, workhorse, limited resolution

Multi Wire Proportional Chamber for slow extr. : gas ionization, limited resol.

- Wire scanner: emission of electrons, workhorse, scanning method
- Ionization Profile Monitor:
  secondary particle detection from interaction beam-residual gas
- Optical Transition Radiation:
  crossing optical boundary, for relativistic beams only
- Synchrotron Light Monitors
  photon detection of emitted synchrotron light in optical and x-ray range
- Summary

An electron bent (i.e. accelerated) by a dipole magnet emit synchrotron light.

This light is emitted into a cone of opening $2/\gamma$ in lab-frame.
⇒Well suited for rel. e^-
For protons:
Only for energies E_{kin} > 100 GeV

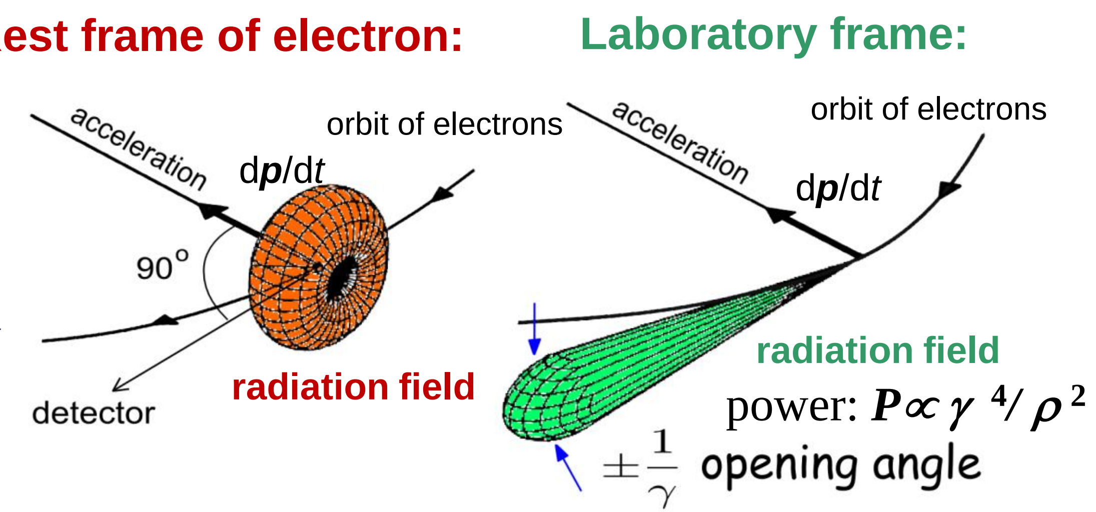

The light is focused to a intensified CCD.

Advantage:
Signal anyhow available!

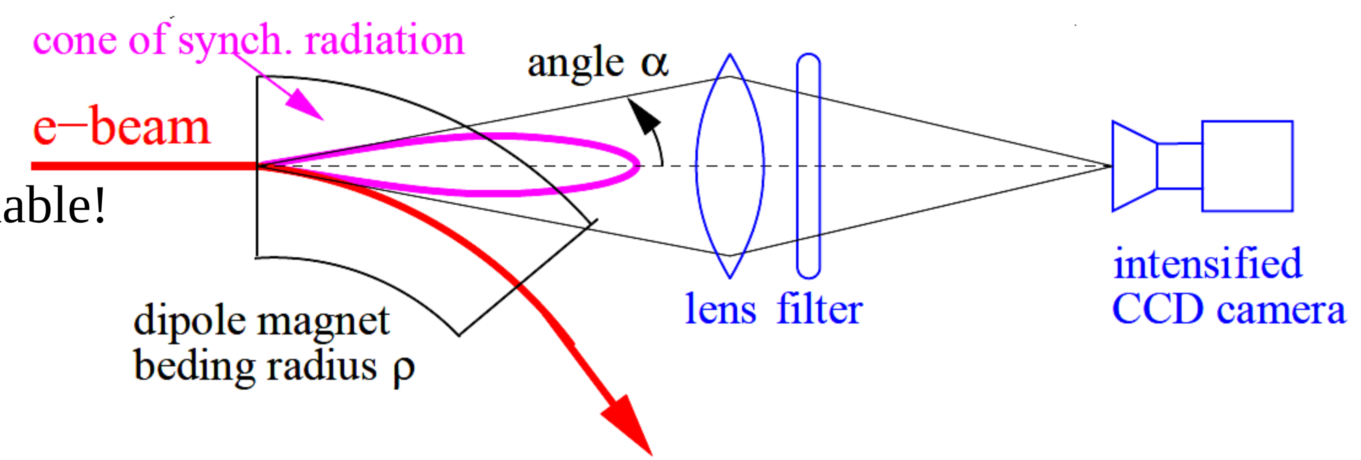

Extracting out of the beam's plane by a (cooled) mirror

→ Focus to a slit + wavelength filter for optical wavelength

→ Image intensified CCD camera

Example: CERN LEP-monitor with bending radius 3.1 km (blue or near UV)

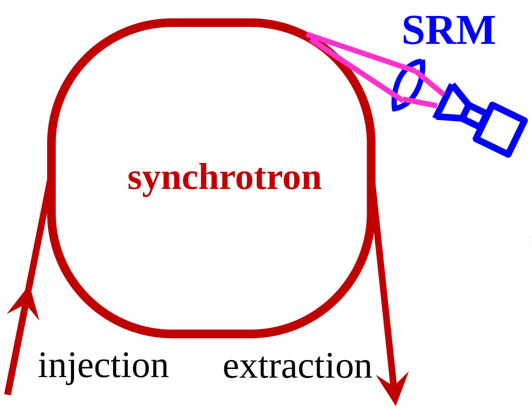

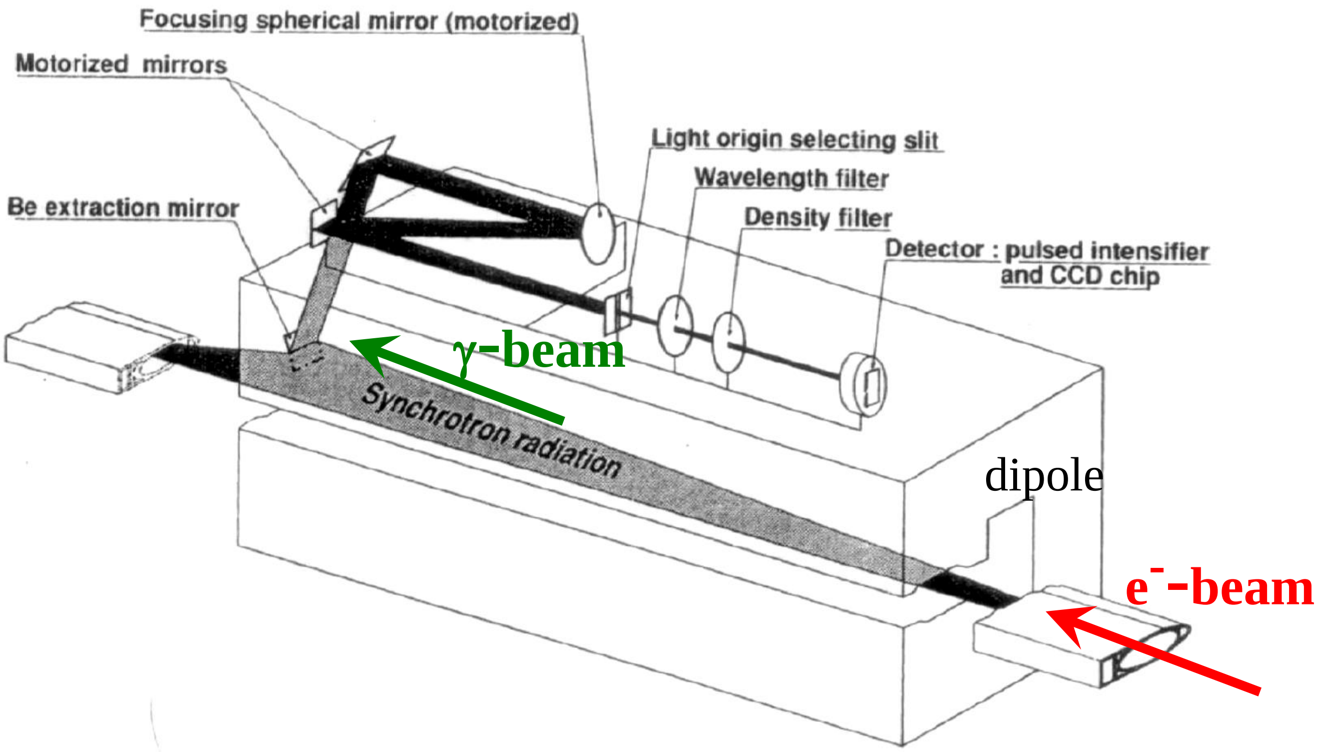

Courtesy C. Bovet (CERN) et al., PAC'91

Result from a Synchrotron Light Monitor

Example: Synchrotron radiation facility APS accumulator ring and blue wavelength:

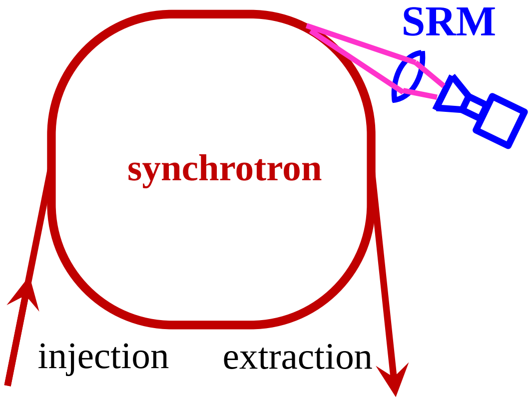

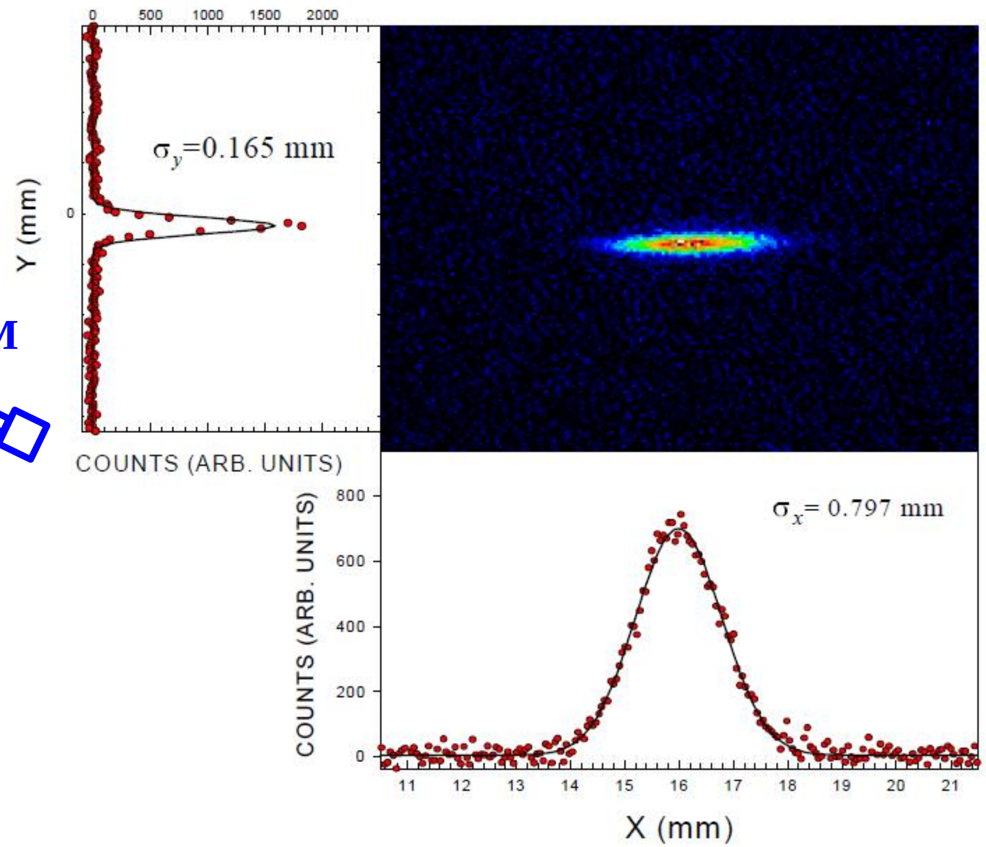

Courtesy
B.X. Yang (ANL) et al.
PAC'97

Advantage: Direct measurement of 2-dim distribution, only mirror installed in the vacuum pipe

Realization: Optics outside of vacuum pipe

Disadvantage: Resolution limited by the diffraction due to finite apertures in the optics.

Limitations:
Diffraction limits the resolution due to Fraunhofer diffraction

$$\Rightarrow \sigma \cong 0.6 \cdot \left(\lambda^2 / \rho\right)^{1/3}$$

$$\approx 100 \ \mu\text{m for typical case}$$

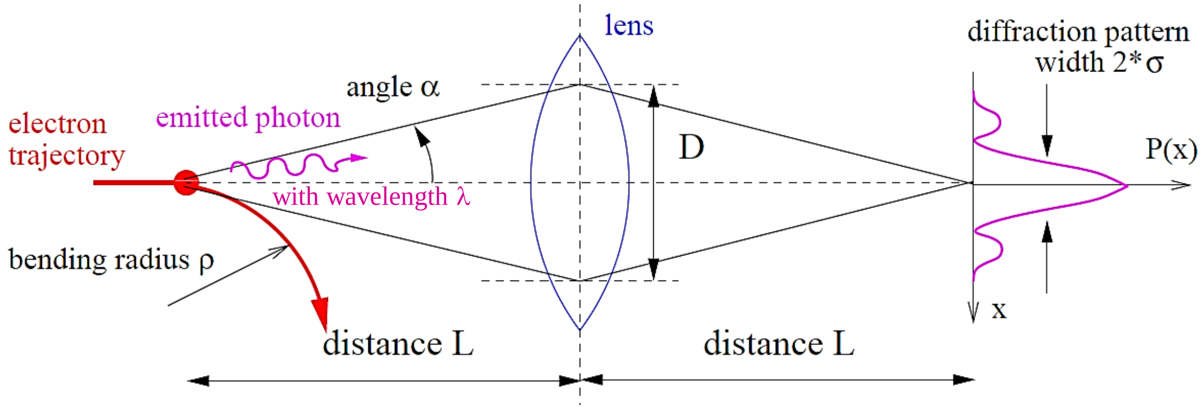

Improvements:

- ***Shorter wavelength:***
  Using x-rays and an aperture of Ø 1mm
  → 'x-ray pin hole camera',
  achievable resolution $\sigma \approx 10$ μm
- ***Interference technique:***
  At optical wavelength
  using a double slit
  → interference fringes
  achievable resolution $\sigma \approx 1$ μm.

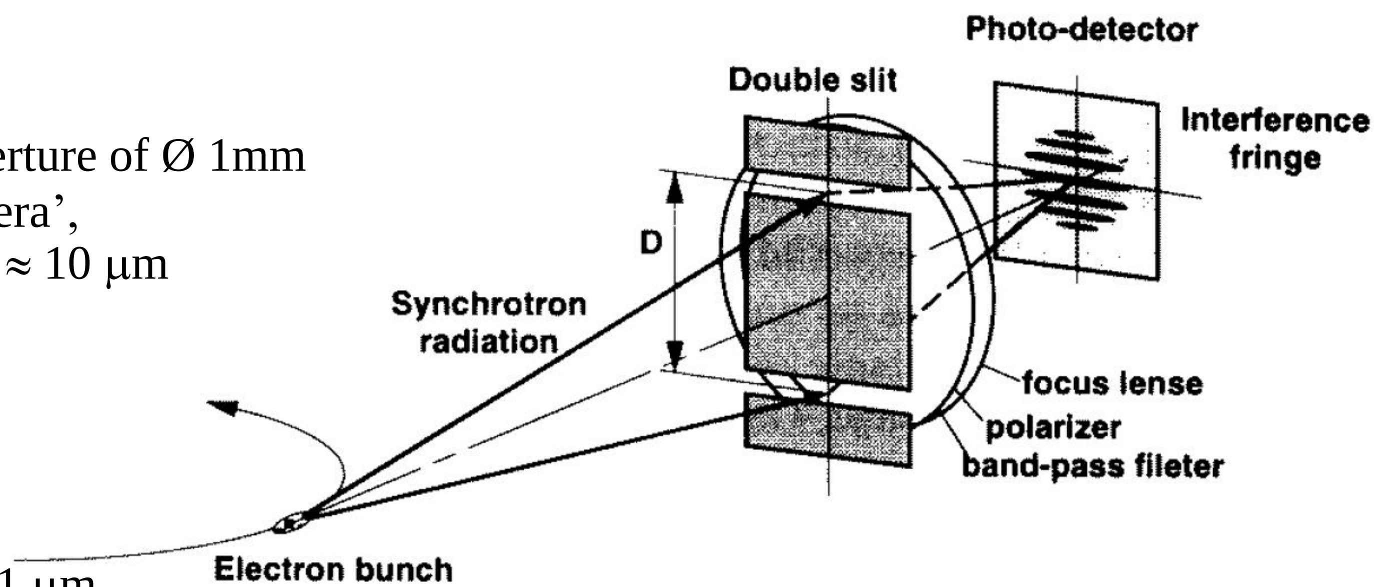

Different techniques are suited for different beam parameters:

e^--beam: typically Ø 0.1 to 3 mm, **protons:** typically Ø 3 to 30 mm

Intercepting ↔ non-intercepting methods

Direct observation of electrodynamics processes:

- Optical synchrotron radiation monitor: non-destructive, for e^--beams, complex, limited res.
- X-ray synchrotron radiation monitor: non-destructive, for e^--beams, very complex
- OTR screen: nearly non-destructive, large relativistic γ needed, e^--beams mainly

Detection of secondary photons, electrons or ions:

- Scintillation screen: destructive, large signal, simple setup, all beams
- Ionization profile monitor: non-destructive, expensive, limited resolution, for protons
- Residual fluorescence monitor: non-destructive, limited signal strength, for protons

Wire based electronic methods:

- SEM-grid: partly destructive, large signal and dynamic range, limited resolution
- Wire scanner: partly destructive, large signal and dynamics, high resolution, slow scan.

Measurement of transverse Emittance

The emittance characterizes the whole beam quality, assuming linear behavior as described by second order differential equation.

It is defined within the phase space as: $\varepsilon_x = \frac{1}{\pi} \int_A dx dx'$

The measurement is based on determination of:

either profile width $\boldsymbol{\sigma_x}$ and angular width $\boldsymbol{\sigma_x'}$ at one location
or $\boldsymbol{\sigma_x}$ at different locations and linear transformations.

Different devices are used at transfer lines:

- Lower energies $\boldsymbol{E_{kin}}$ < 100 MeV/u: slit-grid device, pepper-pot (suited in case of non-linear forces).
- All beams: Quadrupole variation, 'three grid' method using linear transformations (**not** well suited in the presence of non-linear forces)

Synchrotron: lattice functions results in stability criterion

$\Rightarrow$ beam width delivers emittance: $\varepsilon_x = \frac{1}{\beta_x(s)}\left[\sigma_x^2 - \left(D(s)\frac{\Delta p}{p}\right)\right]$ and $\varepsilon_y = \frac{\sigma_y^2}{\beta_y(s)}$

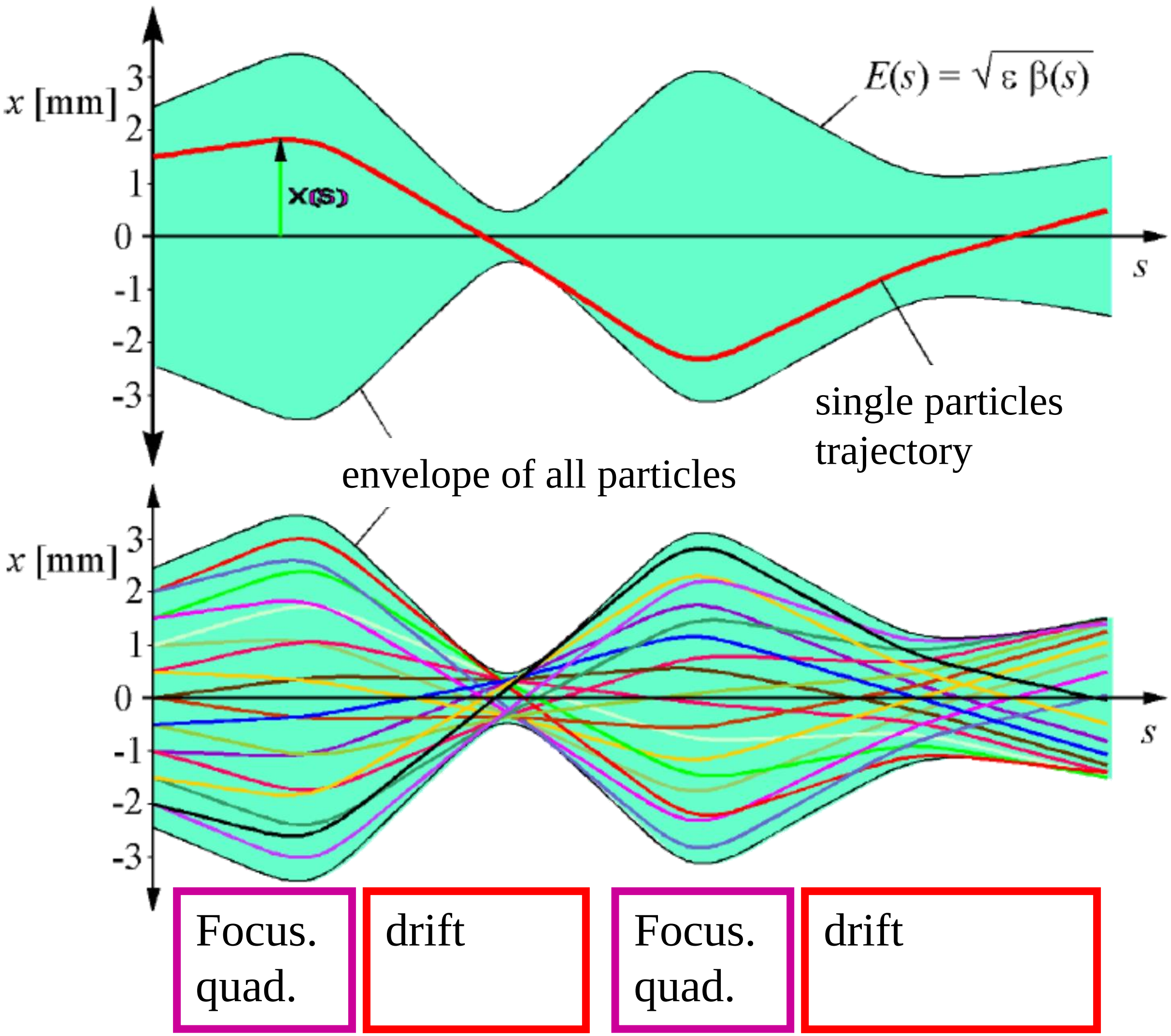

- Single particle trajectories are forming a beam
- They have a distribution of start positions and angles

⇒ Characteristic quantity is the **beam envelope**

- **Goal:**

Transformation of envelope ⇔ behavior of whole ensemble

Courtesy K.Wille

The basic vector is 6 dimensional:

$$\vec{x}(s) = \begin{pmatrix} x \\ x' \\ y \\ y' \\ l \\ \delta \end{pmatrix} = \begin{pmatrix} \text{hori. spatial deviation} \\ \text{horizontal divergence} \\ \text{vert. spatial deviation} \\ \text{vertical divergence} \\ \text{longitudinal deviation} \\ \text{momentum deviation} \end{pmatrix} = \begin{pmatrix} [\text{mm}] \\ [\text{mrad}] \\ [\text{mm}] \\ [\text{mrad}] \\ [\text{mm}] \\ [‰] \end{pmatrix}$$

The transformation of a single particle from a location s_0 to s_1 is given by the Transfer Matrix R:

$$\vec{x}(s_1) = \mathrm{R}(s) \cdot \vec{x}(s_0)$$

The transformation of a the envelope from a location s_0 to s_1 is given by the Beam Matrix σ:

$$\sigma(s_1) = \mathrm{R}(s) \cdot \sigma(s_0) \cdot \mathrm{R}^T(s)$$

6-dim Beam Matrix

with *decoupled*

hor. & vert. plane:

$$\sigma = \begin{pmatrix} \sigma_{11} & \sigma_{12} & 0 & 0 & \sigma_{15} & \sigma_{16} \\ \sigma_{12} & \sigma_{22} & 0 & 0 & \sigma_{25} & \sigma_{26} \\ 0 & 0 & \sigma_{33} & \sigma_{34} & 0 & 0 \\ 0 & 0 & \sigma_{34} & \sigma_{44} & 0 & 0 \\ \sigma_{15} & \sigma_{25} & 0 & 0 & \sigma_{55} & \sigma_{56} \\ \sigma_{16} & \sigma_{26} & 0 & 0 & \sigma_{56} & \sigma_{66} \end{pmatrix}$$

Horizontal beam matrix:

$$\sigma_{11} = \langle x^2 \rangle$$

$$\sigma_{12} = \langle x \cdot x' \rangle$$

$$\sigma_{22} = \langle x'^2 \rangle$$

Beam width for the three coordinates:

$$x_{rms} = \sqrt{\sigma_{11}}$$

$$y_{rms} = \sqrt{\sigma_{33}}$$

$$l_{rms} = \sqrt{\sigma_{55}}$$

The emittance characterizes the whole beam quality: $\varepsilon_x = \frac{1}{\pi}\int_A dxdx'$

Ansatz:

Beam matrix at one location: $\boldsymbol{\sigma} = \begin{pmatrix} \sigma_{11} & \sigma_{12} \\ \sigma_{12} & \sigma_{22} \end{pmatrix} = \varepsilon \cdot \begin{pmatrix} \beta & -\alpha \\ -\alpha & \gamma \end{pmatrix}$ with $\vec{x} = \begin{pmatrix} x \\ x' \end{pmatrix}$

It describes a 2-dim probability distr.

The value of emittance is:

$$\varepsilon_x = \sqrt{\det \boldsymbol{\sigma}} = \sqrt{\sigma_{11}\sigma_{22} - \sigma_{12}^2}$$

For the profile and angular measurement:

$$x_\sigma = \sqrt{\sigma_{11}} = \sqrt{\varepsilon\beta} \quad \text{and}$$

$$x'_\sigma = \sqrt{\sigma_{22}} = \sqrt{\varepsilon\gamma}$$

Geometrical interpretation:

All points $\boldsymbol{x}$ fulfilling $\boldsymbol{x}^t \cdot \boldsymbol{\sigma}^{-1} \cdot \boldsymbol{x} = 1$ are located on a **ellipse**

$$\boldsymbol{\sigma_{22}x^2 - 2\sigma_{12}xx' + \sigma_{11}x'^2} = \det \boldsymbol{\sigma} = \boldsymbol{\varepsilon_x^2}$$

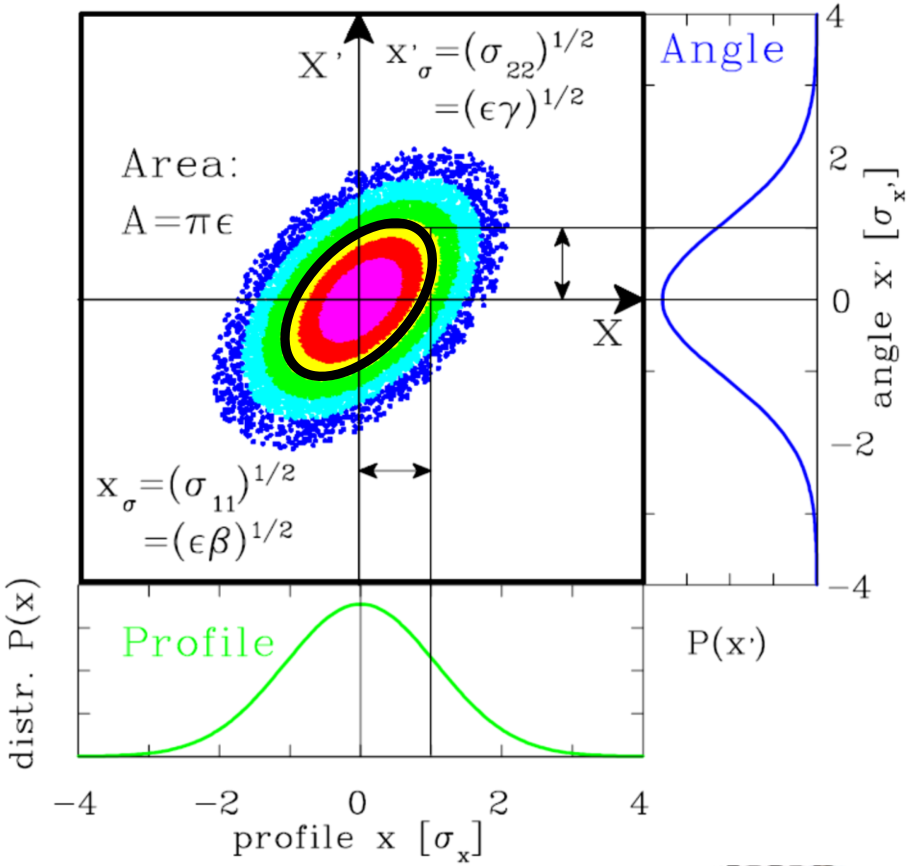

The beam distribution can be non-Gaussian, e.g. at:

- beams behind ion source
- space charged dominated beams at LINAC & synchrotron
- cooled beams in storage rings

General description of emittance

using terms of 2-dim distribution:

Variances

Covariance
i.e. correlation

$$\varepsilon_{rms} = \sqrt{\langle x^2 \rangle \langle x'^2 \rangle - \langle xx' \rangle^2}$$

It describes the value for 1 stand. derivation

For Gaussian beams only:

ε_{rms} ↔ interpreted as area containing a fraction ***f*** of ions: $\varepsilon(f) = -2\pi\varepsilon_{rms} \cdot \ln(1-f)$

factor to ϵ_{rms}	$1 \cdot \epsilon_{rms}$	$\pi \cdot \epsilon_{rms}$	$2\pi \cdot \epsilon_{rms}$	$4\pi \cdot \epsilon_{rms}$	$6\pi \cdot \epsilon_{rms}$	$8\pi \cdot \epsilon_{rms}$
faction of beam f [%]	15	39	63	86	95	98

Care: no common definition of emittance concerning the fraction ***f***

Outline:

- Definition and some properties of transverse **emittance**
- **Slit-Grid device: scanning method**

  scanning slit → beam position & grid → angular distribution
- **Quadrupole strength variation and position measurement**
- **Summary**

Slit-Grid: Direct determination of position and angle distribution.

Used for protons/heavy ions with E_{kin} < 100 MeV/u ⇒ range R < 1 cm.

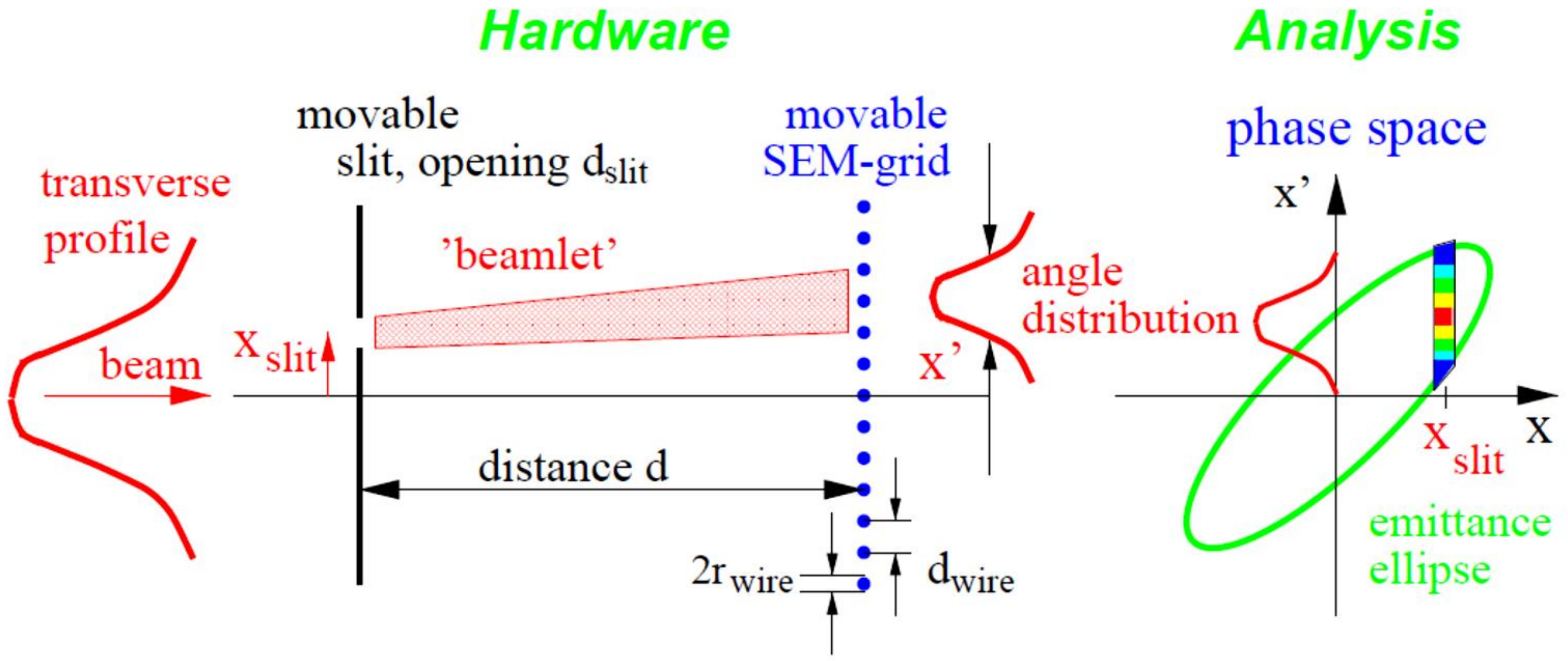

Slit: position ***P(x)*** with typical width: 0.1 to 0.5 mm

Distance: 10 cm to 1 m (depending on beam velocity)

SEM-Grid: angle distribution ***P(x')***

Slit & SEM-Grid

Slit with e.g. 0.1 mm thickness

→ Transmission only from Δx.

Example: Slit of width 0.1 mm (defect)

Moved by stepping motor, 0.1 mm resolution

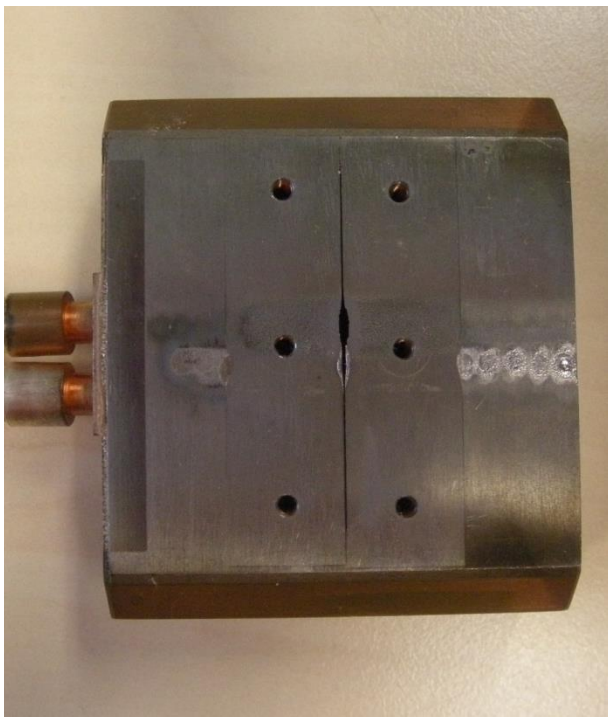

Beam surface interaction: e^- emission

→ measurement of current.

Example: 15 wire spaced by 1.5 mm:

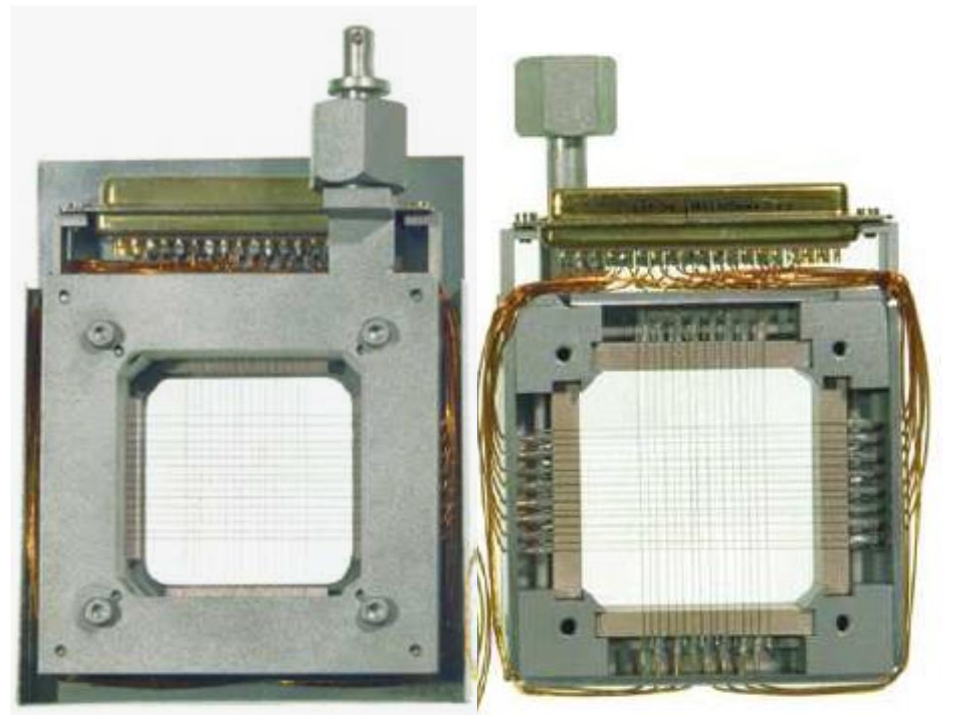

Each wire is equipped with one I/U converter

different ranges settings by R_i

→ very large dynamic range up to 10^6.

The distribution of the ions is depicted as a function of
- Position [mm]
- Angle [mrad]

The distribution can be visualized by
- Mountain plot
- Contour plot

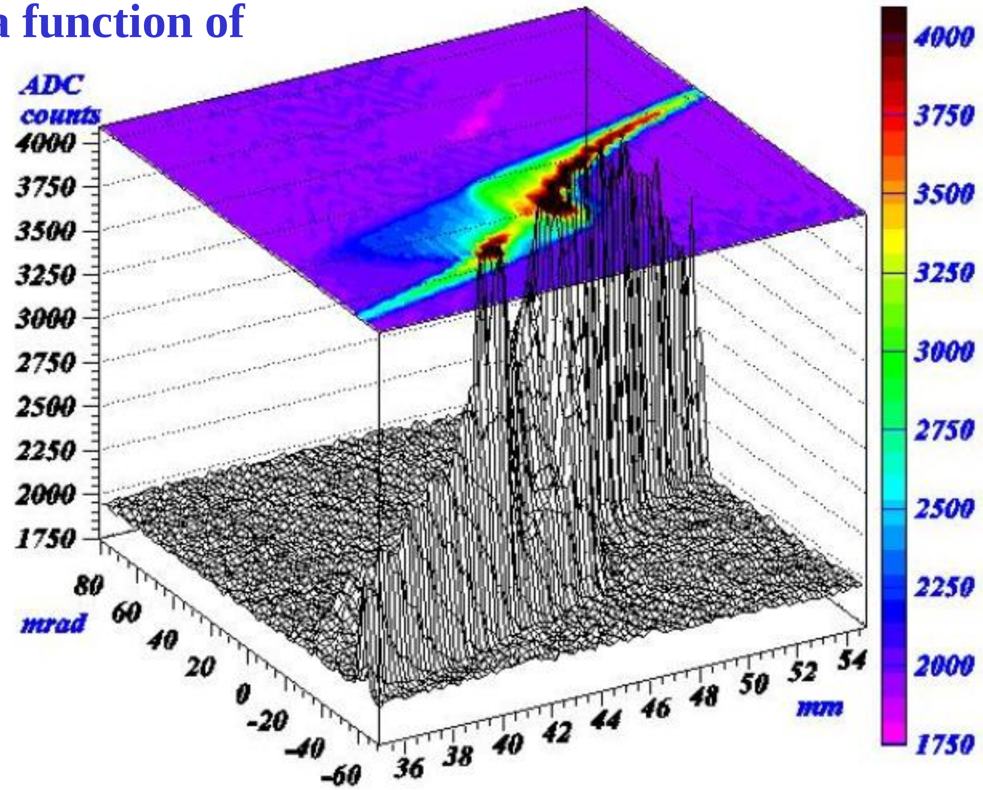

Calc. of 2nd moments <x^2> , <x'^2> & <xx'>

Emittance value ε_{rms} from

$$\varepsilon_{rms} = \sqrt{\langle x^2\rangle\langle x'^2\rangle - \langle xx'\rangle^2}$$

⇒ **Problems:**

- Finite **binning** results in limited resolution
- **Background** → large influence on **<x^2>, <x'^2>** and **<xx'>**

Or fit of distribution with an ellipse

⇒ **Effective emittance only**

Beam: Ar^{4+}, 60 KeV, 15 μA

at Spiral2 Phoenix ECR source.

Plot from P. Ausset, DIPAC 2009

Outline:

- ➢ Definition and some properties of transverse emittance
- ➢ Slit-Grid device: scanning method

  scanning slit → beam position & grid → angular distribution
- ➢ Quadrupole strength variation and position measurement

  emittance from several profile measurement and beam optical calculation
- ➢ Summary

From a profile determination, the emittance can be calculated via linear transformation, if a well known and constant distribution (e.g. Gaussian) is assumed.

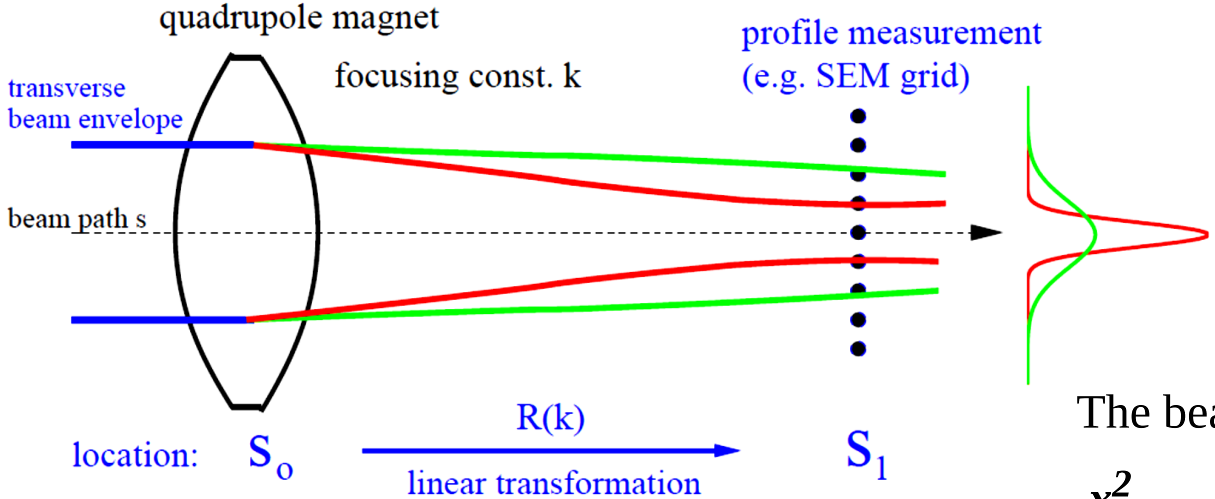

The beam width x_{max} and

$x^2_{max} = \sigma_{11}(1, k)$ is measured,

matrix **R(k)** describes the focusing.

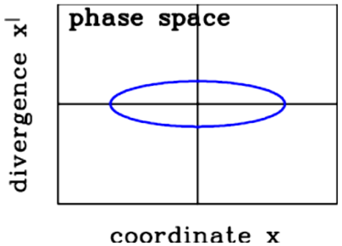

beam matrix:

(Twiss parameters)

$\sigma_{11}(0)$, $\sigma_{12}(0)$, $\sigma_{22}(0)$

to be determined

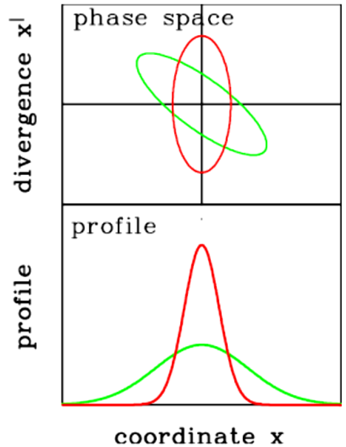

measurement:

$x^2(k) = \sigma_{11}(1,k)$

Emittance Measurement by Quadrupole Variation

- The beam width x_{max} at s_1 is measured, and therefore $\sigma_{11}(1,k_i) = x^2_{max}(k_i)$.
- Different focusing of the quadrupole $k_1, k_2 ... k_n$ is used: $\Rightarrow \mathbf{R}_{\mathbf{focus}}(k_i)$, including the drift, the transfer matrix is changed $\mathbf{R}(k_i) = \mathbf{R}_{\mathbf{drift}} \cdot \mathbf{R}_{\mathbf{focus}}(k_i)$.
- Task: Calculation of *beam* matrix $\sigma(0)$ at entrance s_0 (size and orientation of ellipse)
- The transformations of the beam matrix are: $\sigma(1,k) = \mathbf{R}(k) \cdot \sigma(0) \cdot \mathbf{R}^{\mathbf{T}}(k)$.

$\Longrightarrow$ Resulting in a redundant system of linear equations for $\sigma_{ij}(0)$:

$$\begin{aligned}
\sigma_{11}(1,k_1) &= R^2_{11}(k_1)\cdot\sigma_{11}(0) + 2R_{11}(k_1)R_{12}(k_1)\cdot\sigma_{12}(0) + R^2_{12}(k_1)\cdot\sigma_{22}(0) \quad \text{focusing } k_1 \\
&\vdots \\
\sigma_{11}(1,k_n) &= R^2_{11}(k_n)\cdot\sigma_{11}(0) + 2R_{11}(k_n)R_{12}(k_n)\cdot\sigma_{12}(0) + R^2_{12}(k_n)\cdot\sigma_{22}(0) \quad \text{focusing } k_n
\end{aligned}$$

- To learn something on possible errors, $n > 3$ settings have to be performed. A setting with a focus close to the SEM-grid should be included to do a good fit.

- *Assumptions:*
  - Only elliptical shaped emittance can be obtained.
  - No broadening of the emittance e.g. due to space-charge forces.
  - If *not* valid: A self-consistent algorithm has to be used.

Using the 'thin lens approximation' i.e. the quadrupole has a focal length of ***f***:

$$\mathrm{R}_{focus}(K) = \begin{pmatrix} 1 & 0 \\ -1/f & 1 \end{pmatrix} \equiv \begin{pmatrix} 1 & 0 \\ K & 1 \end{pmatrix} \Rightarrow \mathrm{R}(L,K) = \mathrm{R}_{drift}(L)\cdot \mathrm{R}_{focus}(K) = \begin{pmatrix} 1+LK & L \\ K & 1 \end{pmatrix}$$

Measurement of **σ(*1,K*) = R(*K*)·σ(*0*)·R^T(*K*)**

Example: Square of the beam width at ELETTRA 100 MeV e$^-$ Linac, YAG:Ce:

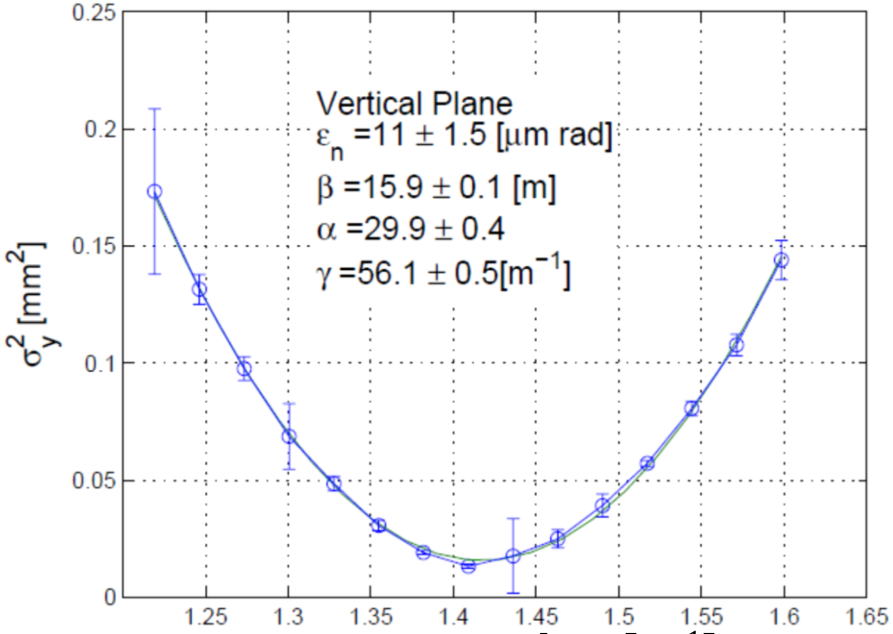

Focusing strength K [m^{-1}]

G. Penco (ELETTRA) et al., EPAC'08

For completeness: The relevant formulas

$$\sigma_{11}(1,K) = L^2\sigma_{11}(0)\cdot K^2 + 2\cdot(\; L\sigma_{11}(0) + L^2\sigma_{12}(0)\;)\cdot K + L^2\sigma_{22}(0) + \sigma_{11}(0)$$

$$\equiv a\cdot K^2 \; - \; 2ab\cdot K \; + \; ab^2 + c$$

The σ-matrix at quadrupole is:

$$\sigma_{11}(0) = \frac{a}{L^2}$$

$$\sigma_{12}(0) = -\frac{a}{L^2}\left(\frac{1}{L} + b\right)$$

$$\sigma_{22}(0) = \frac{1}{L^2}\left(ab^2 + c + \frac{2ab}{L} + \frac{a}{L^2}\right)$$

$$\epsilon = \sqrt{\det \sigma(0)} = \sqrt{\sigma_{11}(0)\sigma_{22}(0) - \sigma_{12}^2(0)} = \sqrt{ac}/L^2$$

Instead of quadrupole variation, the beam width is measured at ***different*** locations:

The procedure is:

- Beam width $x(i)$ measured at the locations s_i
  $\Rightarrow$ beam matrix element $x^2(i) = \sigma_{11}(i)$.
- The transfer matrix $\mathbf{R}(i)$ is known. (without dipole a 3 × 3 matrix.)
- The transformations are:
  $\boldsymbol{\sigma}(i) = \mathbf{R}(i)\boldsymbol{\sigma}(0)\mathbf{R}^T(i)$
  $\Rightarrow$ redundant equations:

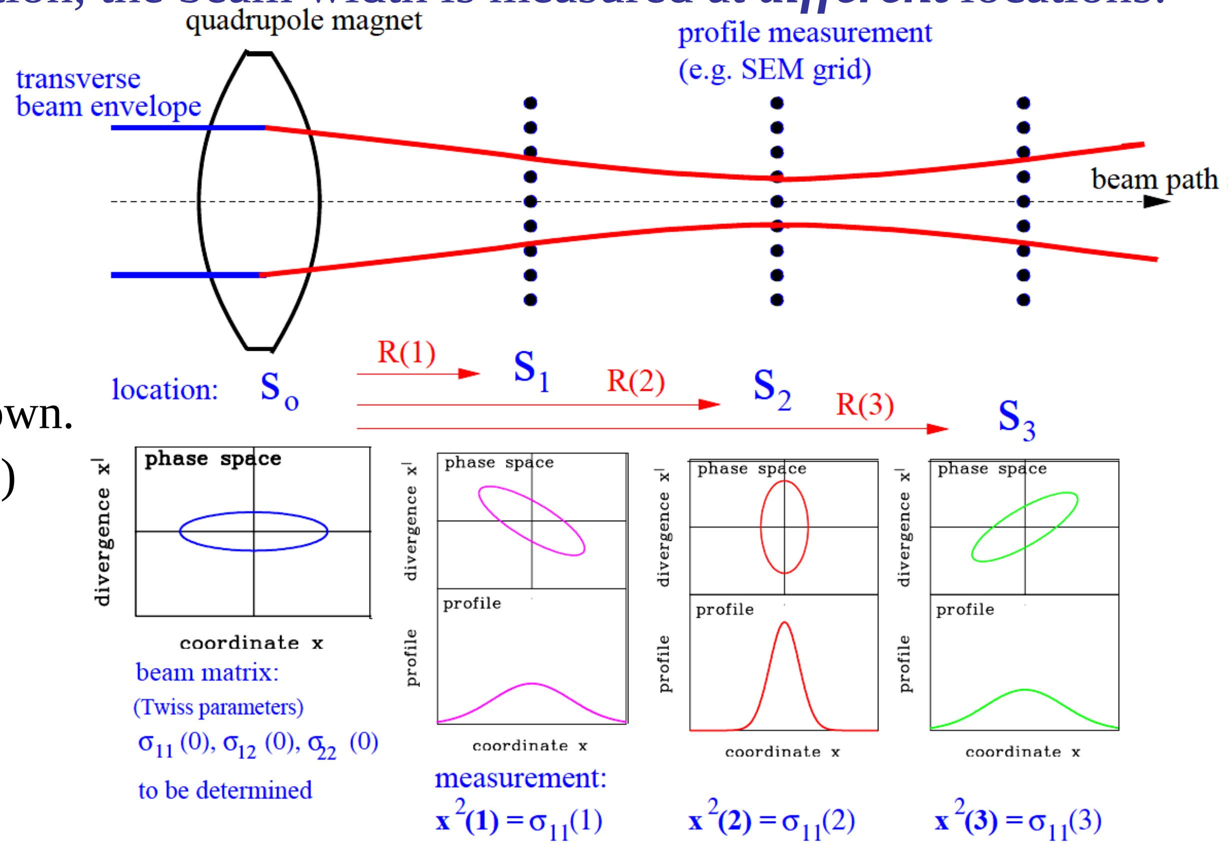

$$
\begin{aligned}
\sigma_{11}(1) &= R_{11}^2(1)\cdot\sigma_{11}(0) + 2R_{11}(1)R_{12}(1)\cdot\sigma_{12}(0) + R_{12}^2(1)\cdot\sigma_{22}(0) && \mathbf{R}(1): s_0 \rightarrow s_1 \\
\sigma_{11}(2) &= R_{11}^2(2)\cdot\sigma_{11}(0) + 2R_{11}(2)R_{12}(2)\cdot\sigma_{12}(0) + R_{12}^2(2)\cdot\sigma_{22}(0) && \mathbf{R}(2): s_0 \rightarrow s_2 \\
&\vdots \\
\sigma_{11}(n) &= R_{11}^2(n)\cdot\sigma_{11}(0) + 2R_{11}(n)R_{12}(n)\cdot\sigma_{12}(0) + R_{12}^2(n)\cdot\sigma_{22}(0) && \mathbf{R}(n): s_0 \rightarrow s_n
\end{aligned}
$$

Solution: Solving the linear equations like for quadrupole variation or fitting the profiles with linear optics code (e.g. MADX, TRANSPORT, Mirko).

Example: The hor. and vert. beam envelope and the beam width at a transfer line:

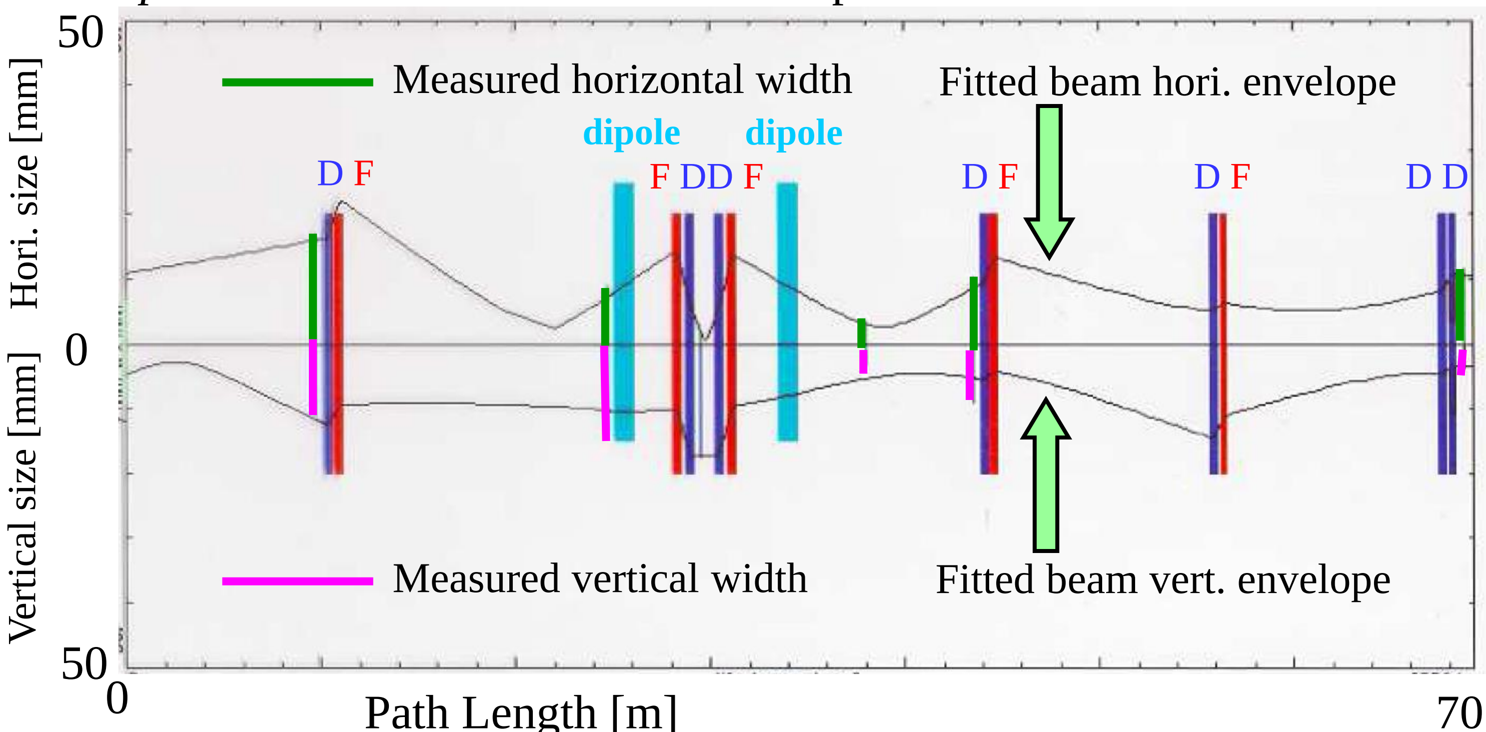

Assumptions: ➢ constant emittance, in particular no space-charge broadening

➢100 % transmission i.e. no loss due to vacuum pipe scraping

➢ no misalignment, i.e. beam center equals center of the quadrupoles.

Summary for transverse Emittance Measurement

Emittance is the important quantity for comparison to theory.

It includes size (value of ε) and orientation in phase space (**σ_{ij}** or **α, β** and **γ**)

(three independent values $\varepsilon_{rms} = \sqrt{\sigma_{11} \cdot \sigma_{22} - \sigma_{12}} = \sqrt{< x^2 > \cdot < x'^2 > - < xx' >^2}$

assuming no coupling between horizontal, vertical and longitudinal planes)

Transfer line, low energy beams → direct measurement of x- and x′-distribution

- ***Slit-grid:*** movable slit → ***x***-profile, grid → ***x′***-profile

Transfer line, all beams → profile measurement + linear transformation:

- ***Quadrupole variation:*** one location, different setting of a quadrupole
- ***'Three grid method':*** different locations
- ***Assumptions:***
  - well aligned beam, no steering
  - no emittance blow-up due to space charge.

Remark: For a synchrotron with a stable beam,
width measurement is sufficient using $x_{rms} = \sqrt{\varepsilon_{rms} \cdot \beta}$

Thank you for your attention!

Backup slides

Influence of the residual gas ion trajectory by :

- External electric field $\boldsymbol{E_{ex}}$
- Electric field of the beam's space charge $\boldsymbol{E_{space}}$

e.g. Gaussian density distribution for round beam: $E_{space}(r) = \frac{1}{2\pi\varepsilon_0} \cdot \frac{qeN}{l} \cdot \frac{1}{r} \cdot \left[1 - \exp\left(-\frac{r^2}{2\sigma^2}\right)\right]$

Estimation of correction: $\sigma_{corr}^2 \approx \frac{e^2 \ln 2}{4\pi\varepsilon_0 \sqrt{m_p c^2}} \cdot \frac{qN}{l} \cdot d_{gap} \cdot \sqrt{\frac{1}{eU_{ex}}} \propto N \cdot d_{gap} \cdot \sqrt{\frac{1}{U_{ex}}}$

With the measured beam width is given by convolution: $\sigma_{meas}^2 = \sigma_{true}^2 + \sigma_{corr}^2$

Example: U^{73+}, 10^9 particles per 3 m bunch length, cooled beam with $\boldsymbol{\sigma_{true}}$ = 1 mm FWHM.

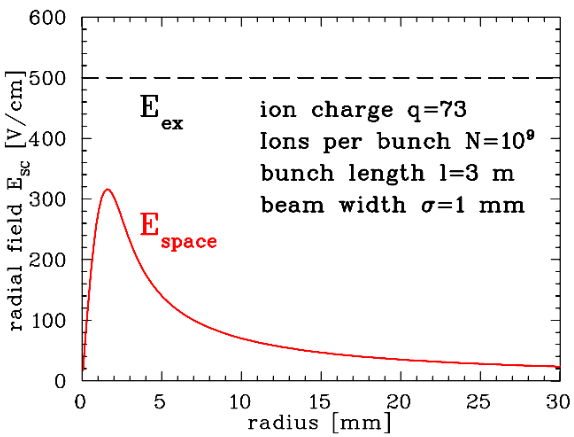

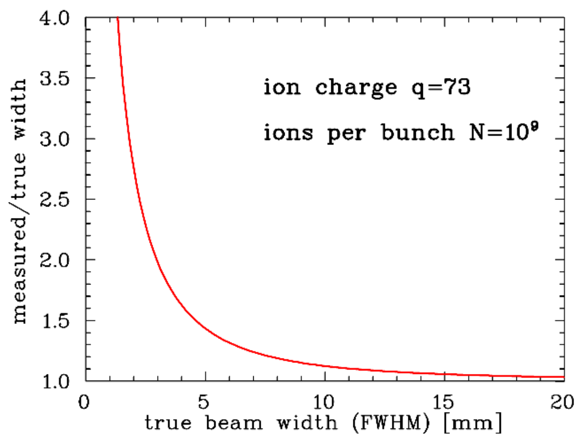

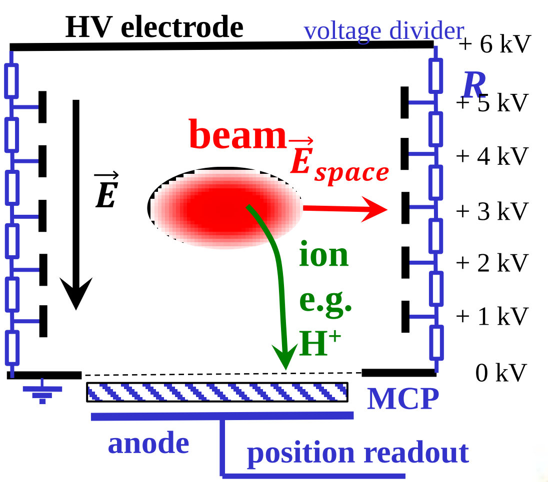

OTR with 45^0 beam incidence and observation at 90^0 :

A charge ***e*** approaches an ideal conducting boundary under 45^0

- image charge is created by electric field
- dipole rotated by 45^0 & deformed due to relativistic field propagation
- penetration of surface within ***t*** < 10 fs: sudden change of sources
- due to reflection on surface emission symmetric around 90^0

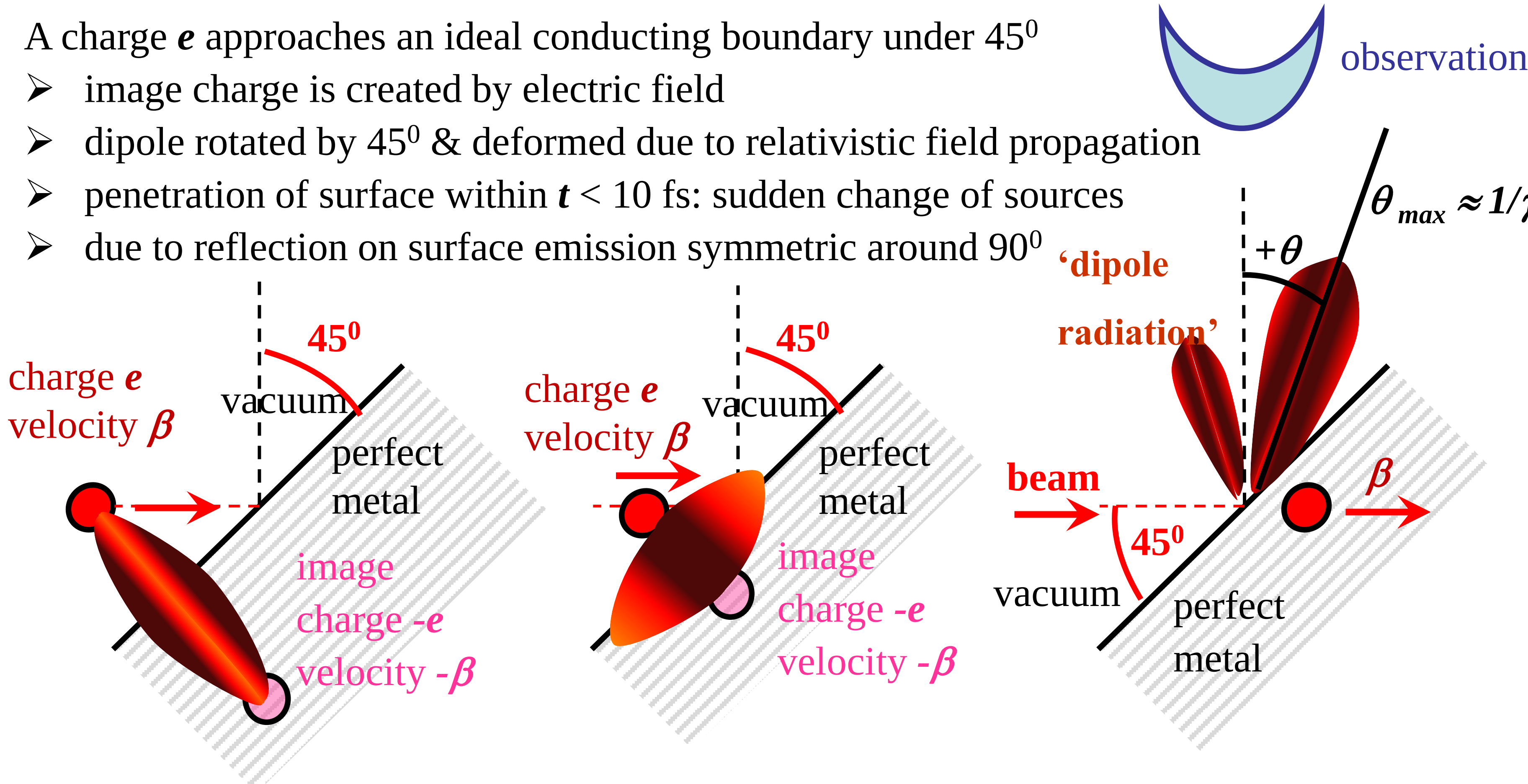

Example: Booster at the light source ALBA acceleration from 0.1 → 3 GeV within 130 ms

Profile measure by synchrotron light monitor:

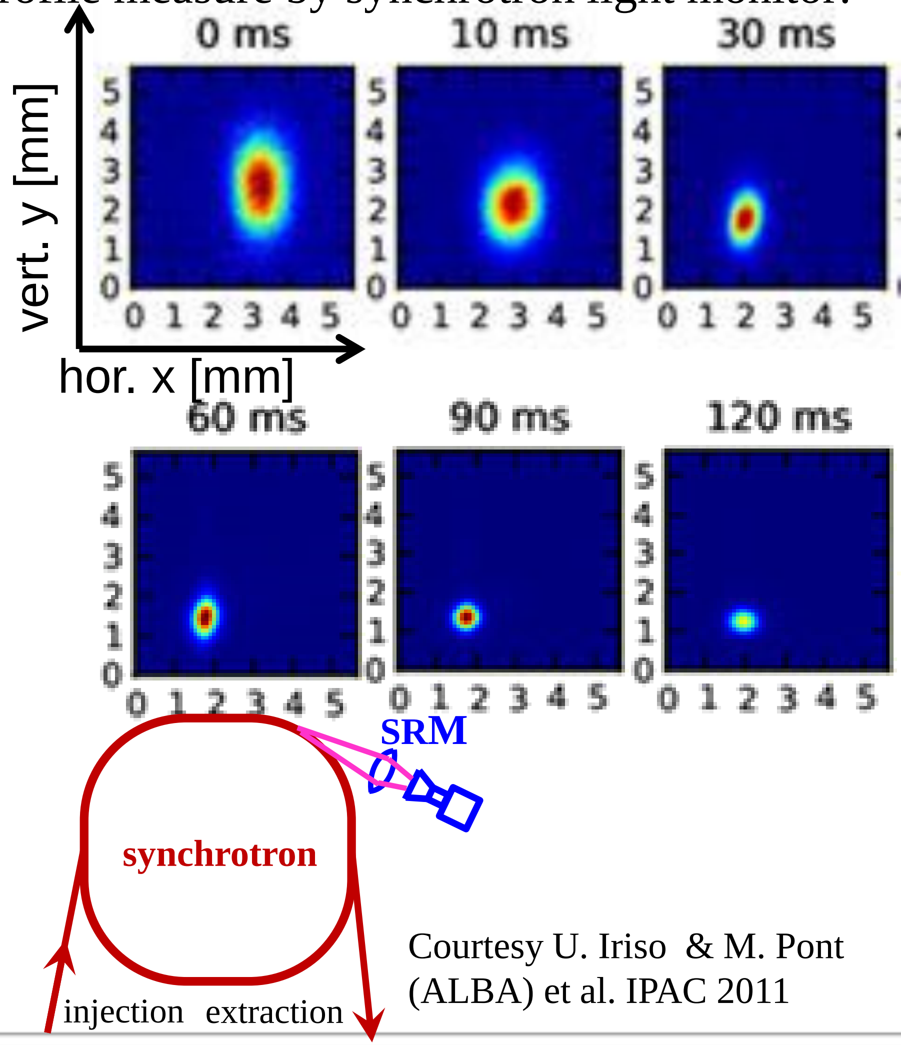

Courtesy U. Iriso & M. Pont (ALBA) et al. IPAC 2011

The beam emittance in influenced by:

- Adiabatic damping
- Longitudinal momentum contribution

  via dispersion $\Delta x_D(s) = D(s) \cdot \frac{\Delta p}{p}$

  total width $\Delta x_{tot}(s) = \sqrt{\varepsilon\beta(s) + D(s) \cdot \frac{\Delta p}{p}}$
- Quantum fluctuation due to light emission